Faculta di Ingegneria civile e industriale

Dipartimento di Ingegneria Astronautica, Elettrica ed Energetica

Corso di Laurea Magistrale in ‘electric machine’

“progettazione di un ingranaggio magnetico”

“Design of a Magnetic Gear”

Laureanda: Yasmina Fezzoui

Relatore : Prof. Guilli.Fabio Capponi

Prof. Rachid Saou

July 2019

The Erasmus experience at sapienza universita di Roma made me discover new horizons, this made me grow, more independent and responsible.

for that i thank all the staff of sapienza universita for having welcomed me, i send my sincere thanks to the staff of the machine lab and my supervisor Professor fabio capponi, who are for me a 2nd family.

I thank the staff of the Department of Electrical Engineering of my home university abderrahmane mira bejaia, and I extend my sincere thanks to my supervisor Professor Rachid Saou.

Finally, what would I be without my parents?

I hope they will be proud of what I have become.

« thank you mom and dad »

Table of Contents

bibliography

[01] C. G. Armstrong, “Power transmitting device,” US Pat. 687 292, 1901.

[02] A. Neuland, “Apparatus for transmitting power,” US Patent 1 171 351, 1916.

[03] G. Reese, “Magnetic gearing arrangement,” US Patent 3 301 091, 1967

[04] J. T.B. Martin, “Magnetic transmission,” US Patent 3 378 710, 1968.

[05]S. Rand, “Magnetic transmission system,” US Patent 3 523 204, 1970

[06] N. Laing, “Magnetic transmission,” US Patent 345 650, 1972.

[07] N.Laing, “Centrifugal pump with magnetic drive,” US Patent 3 762 839, 1973

[08] D. Hesmondhalgh and D. Tipping, “A multielement magnetic gear,” IEEE PROCEEDINGS, vol. 127, 1980

[09] B. Ackermann, “Magnetic drive arrangement,” US Patent 5 994 809, 1999.

[10] B. Ackermann and L. Honds, “Magnetic drive arrangement comprising a plurality of magnetically cooperating parts which are movable relative to one another,” US Patent 5 633 555, 1997 ;

[12] K. Atallah and D. Howe, “A novel high-performance magnetic gear,” IEEE TRANSACTIONS ON MAGNETICS, vol. 37, no. 4, pp. 2844–2846, 2001

[13] F. J. P.O. Rasmussen, T.O. Anderson and O. Nielsen, “Development of a high performance magnetic gear,” in Conference Record of the 38th IAS Annual Meeting in Industry Applications, vol. 3, 2003.

[14] J. W. K. Atallah and D. Howe, “A high-performance linear magnetic gear,” JOURNAL OF APPLIED PHYSICS 97, vol. 10N516, 2005

[15] S. C. J. Rens, K. Atallah and D. Howe, “A novel magnetic harmonic gear,” in IEEE International Electric Machines & Drives Conference IEMDC ’07, 2007

[16] K. Atallah and J. Rens, “Electrical machines,” WO Patent 125 284 A1, 2007 .

[17] K. Atallah, “Magnetic gear,” WO Patent 144 556 A1, 2007.

[18] R. C. J. R. K. Atallah, S. Calverley and D. Howe, “A new pm machine topology for low-speed, high-torque drives,” in Proceedings of the 2008 International Conference on Electrical Machines, 2008.

[19] S. M. K. Atallah, J. Rens and D. Howe, “A novel "pseudo" direct-drive brushless permanent magnet machine,” IEEE TRANSACTIONS ON MAGNETICS, vol. 55, no. 11, pp. 4349–4352, 2008.

[20] Jiabin Wang, Kais Atallah, and S. D. Carvley ‘’A Magnetic Continuously Variable Transmission Device’’ IEEE TRANSACTIONS ON MAGNETICS, VOL. 47, NO. 10, OCTOBER 2011.

[21] Https://en.wikipedia.org/wiki/Magnetic_coupling.

[23] S. Trout, “Rare earth magnet industry in the usa: Current and future trends,” in For the Rare Earth Magnet Workshop, 2002.

[22] K.T. Chau, D. Zhang, J.Z. Jiang, C. Liu, and Y. Zhang, “Design of a magneticgeared outer-rotor permanent-magnet brushless motor for electric vehicles,” IEEE Trans. Magn., vol. 43, no. 6, pp. 2504-2506, Jun. 2007.

[24] L. Jian, K.T. Chau, and J.Z. Jiang, “An integrated magnetic-geared permanent magnet in-wheel motor drive for electric vehicles,” in Proc. IEEE Conf. VPPC 2008, Harbin, China, pp. 1-6.

[25] S. Du, Y. Zhang, and J. Jiang, “Research on a novel combined permanent magnet electrical machine,” in Proc. IEEE Int. Conf. ICEMS 2008, Wuhan, China, pp. 3564-3567.

[26] https://en.wikipedia.org/wiki/Continuously_variable_transmission.

[27] J. Rens and K. Atallah, “Variable Magnetic Gears,” PCT/GB2009/ 000476, publication No. WO/2009/103993, priority date 21.02.2008.

[28] L. X. Xu, Y. Zhang, and X.Wen, “Multi-operational modes and control strategies of dual mechanical port machine for hybrid electrical vehicles,” in *Proc. IEEE Ind. Appl. Soc. 42nd Annu. Meeting*, 2007, pp. 1710–1717.

[29] K. Atallah *et al.*, “Design, analysis and realisation of a high-performance magnetic gear,” *IEE Proc. Elect. Power Appl*, vol. 151, pp. 135–143, 2004.

[30] L. Jian and K. T. Chau, "Design and analysis of a magnetic-geraed electronic-continuously variable transmission system using finite element method," *Progr. Electromagn. Res.*, vol. 107, pp. 47–61, 2010

[31] **Meeker, D. C**., "Finite element method magnetics, version 4.2" (12 Janvier 2016 build), available at : http://www.femm.info.

List of figures

List of tables

Introduction

In the past decade, advances in magnetic gear technology have led to the development of a new class of electrical machine: magnetically geared machines. A magnetically geared machine (MGM) can be defined as an electrical machine, which integrates a magnetic gear (MG), and a conventional permanent magnet (PM) machine in the same volume. What sets these machines a part from other electrical machines is their high torque density. However, this being a new class of electrical machine, there are numerous possibilities and unanswered questions.

These machines – their analysis, design and evaluation – are the subject of this thesis.

In order to fully appreciate the development of magnetically geared machines, an overview of the history of magnetic gears is provided in the following sections and it is explained how a breakthrough in magnetic gear design has led to the development of magnetically geared machines.

Magnetic gears (MGs) offer significant advantages, such as contact-less power transfer, lubricant free operation, inherent over load protection, high torque densities, potential for high efficiency and little or no maintenance.

In the 80s rare earth PMs, especially neodymium-iron-boron ($Nd_2Fe_{14}B$) magnets, started to become commercially available [23]. These rare earth magnets revived the interest in PM machines and magnetic gears. This can be observed in the magnetic gear research activity histogram (see Figure I). The histogram illustrates the number of publications written per year over the last 100 years and reviewed by the researcher. From the figure it can be observed that MGs started to become more popular in the 1990s just after the commercialisation of rare earth PMs.

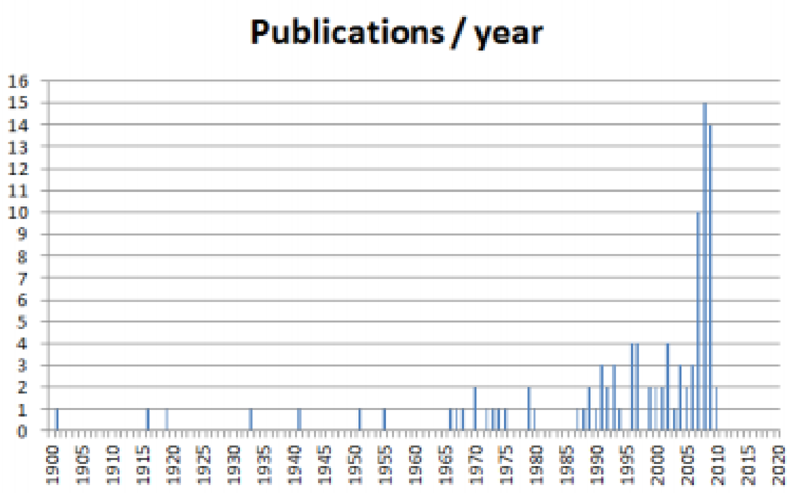

Figure-XXI- magnetic gear histogram

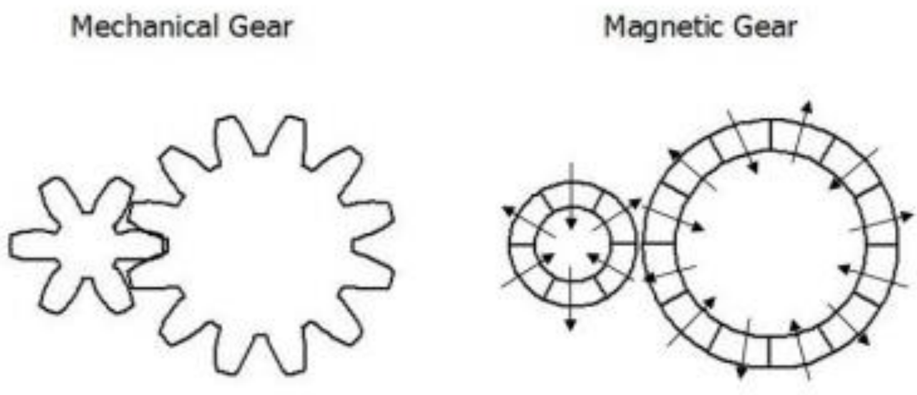

Figure-XXII-comparison between mechanical and magnetic gear

The operating principle of MG is similar to that of mechanical gears, except that all the gear teeth are replaced with magnets, as illustrated in Figure II. The magnetic force between the magnets on the opposing shafts will transfer the force between the shafts in the same way that the gear teeth transfer power by pushing or resisting the opposing teeth.

Chapter 01

I- Magnetic gear history

Armstrong [1] can find the first recorded case of electromagnetic forces being used for geared torque transmission in a patent. Armstrong’s device, shown in Figure III, can be likened to external spur gears. However, instead of torque being transferred from one gear to the next by contacting teeth, the attractive forces transfer torque between the electromagnets on one gear and the ferromagnetic teeth of another gear. Armstrong recognized that this electromagnetic gear did not suffer from mechanical wear and noise generated by contacting teeth. There are two problems with this type of early magnetic gear. Firstly, the torque density is very low because force is only generated in the limited space around the active teeth. Secondly, the torque transmission efficiency is not very high because a large current is required to excite the electromagnetic field. Thus, this type of gear cannot compete with mechanical gears in practical terms.

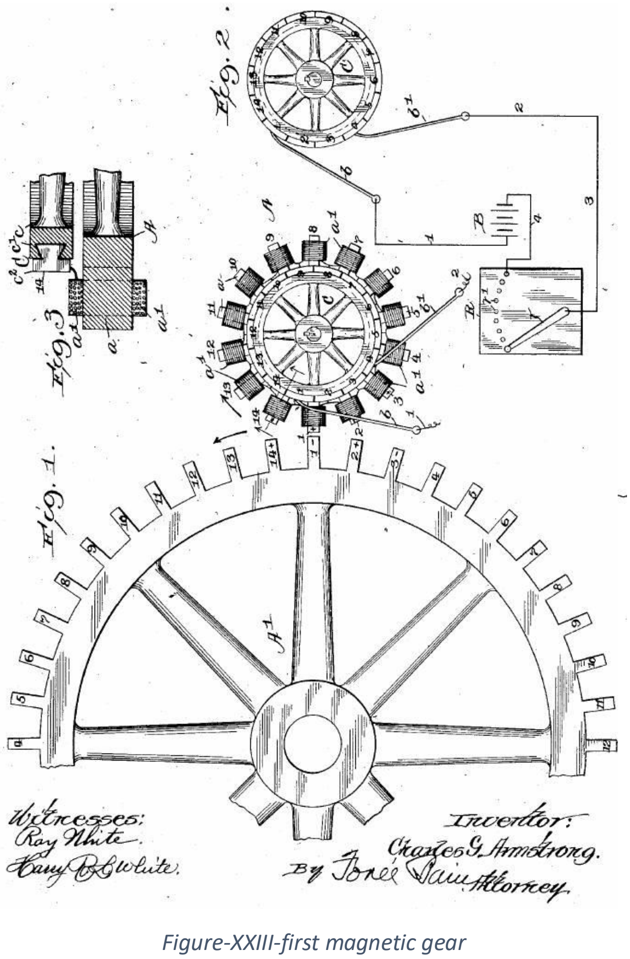

Figure-XXIII-first magnetic gear

In 1916 Neuland [2] invented a far superior magnetic gear. The gear consisted of three main parts, a laminated steel outer- and inner-rotor and magnetic modulation pieces in between the two steel rotors (see Figure IV). The modulation pieces were shaped to modulate magnetic flux so that the inner rotor and the outer rotor saw the correct harmonics in accordance with the number of teeth on each shaft. The ratio of teeth on the outer- and inner-rotor determined the gear ratio between the shafts. The torque density of this configuration was greatly improved compared to the spur-type design from [1], since most of the gear teeth transfered torque at any given moment. The patent also described a few variations on the design. The problem with this design was that there were only magnets on one of the shafts, which led to impractical air-gap sizes.

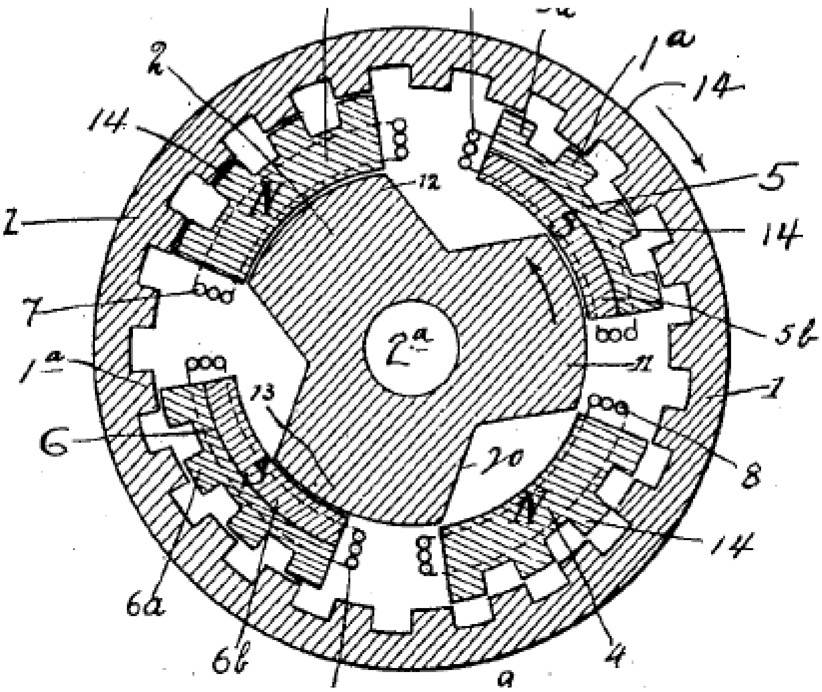

Figure-XXIV-coaxial magnetic gear

In 1967 Reese [03] invented a magnetic gear similar to the one described in [2]. The difference was that the inner rotor contained the PMs (see Figure V for an illustration of the gear). The two outer rotors had a different number of teeth. The inner PM-rotor was the high speed shaft, the middle rotor was the output shaft and the outer rotor was kept stationary. When the inner PMs were rotated, the middle rotor would rotate with it. The magnetic flux of the PM's tended to take the path with the lowest permeability, which is through the steel teeth of the rotors. This made the teeth of the rotor rotate in accordance with the magnetic flux of the PMs. The speed of the rotor then became a function of the ratio of the number of teeth between the rotors and the number of PM poles

In 1968 Martin [04] designed a similar gear as [2] and [03], by replacing the outer rotor with PM's (see Figure VI). The flux-modulator (28) modulated the magnetic flux between the outer- and the inner-rotor.

The operating principle of the flux-modulation can be explained with the help of Figure VII. The right side of each picture represents the PMs on the outer rotor. The middle black pieces represents the flux-modulator and the left side represents the flux content that the inner rotor would interact with. Figure VIIA is an illustration of the inner rotor interacting with a north pole. Figure VIIB is an illustration of what happens when the modulation pieces are moved just by one space and the inner rotor faces a south pole. If the modulation pieces are spaced differently the inner rotor would interact with a north and a south pole (as seen in Figure VIIC). The flux-modulator controls how the two rotors interact with each other. The gear ratio is a function of the number of PM's on both rotors and the number of modulation pieces in the flux modulator. The patent also described a number of designs where the flux-modulator was reconfigured in other configurations, but the same operating principle counted.

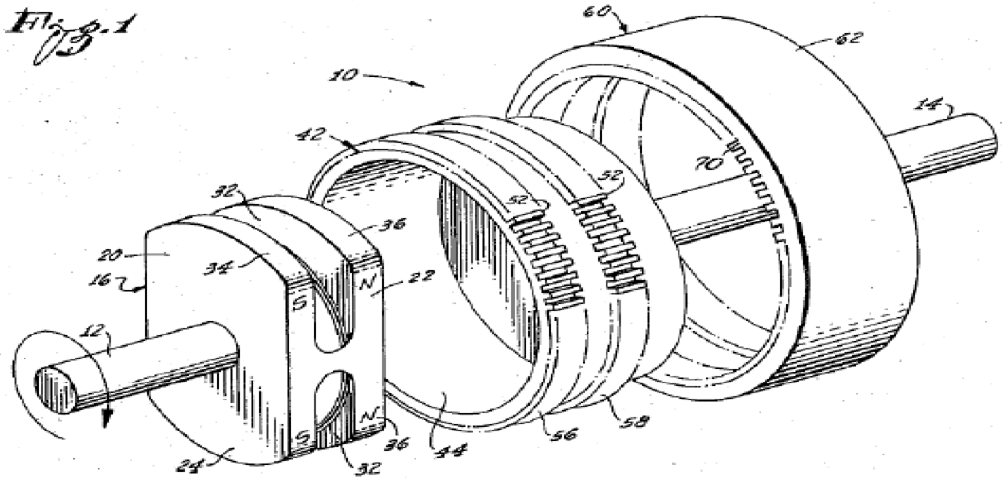

Figure -XXV-coaxial magnetic gear

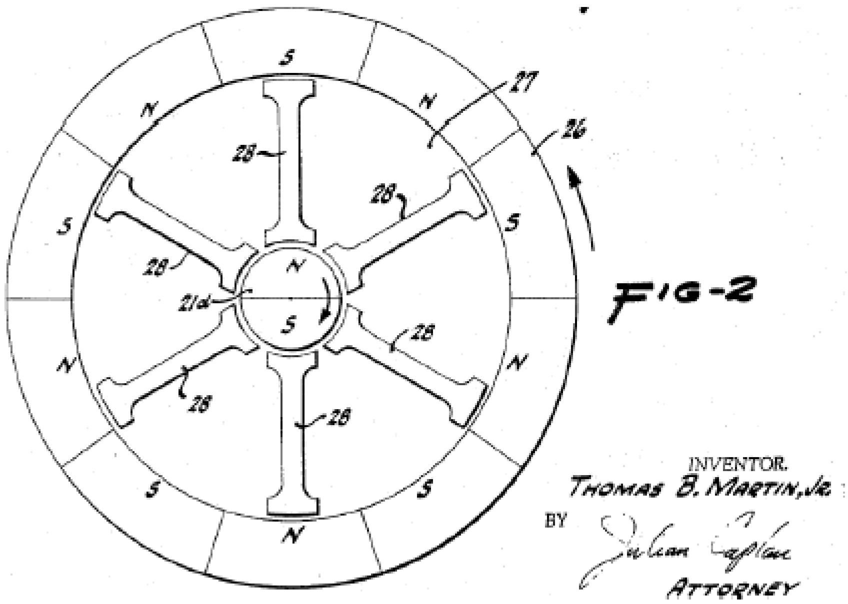

Figure -XXVI-coaxial magnetic gear (shutter type)

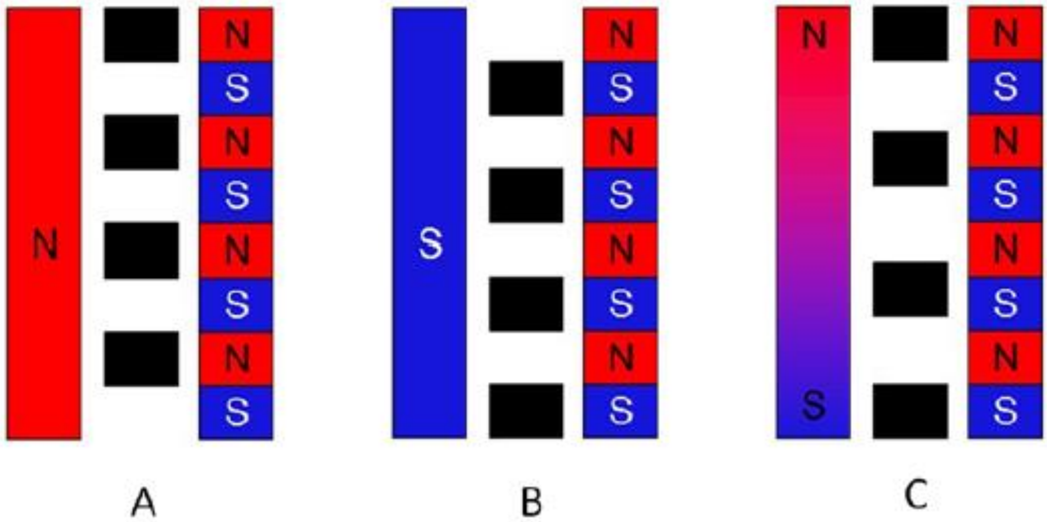

Figure-XXVII-modulation pieces explained

In 1970 Rand [05] took out a patent for a simple spur-type magnetic gear. He designed the PMs so that both the north and south poles of the PMs faced radially outward (see Figure VIII). This increased the amount of magnetic material needed and the cost of manufacturing

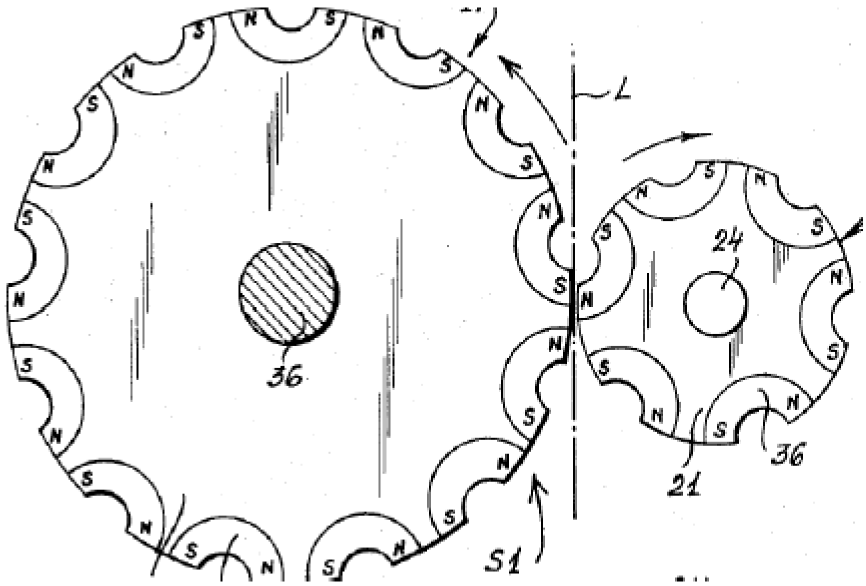

Figure-XXVIII-spur type magnetic gear with U-magnets

In 1972 Laing [06] took out a patent for a magnetic gear very similar to [04] of 1968. The difference was that the flux-modulator in between the PM rotors were a bit different and that only every second pole on the rotors contained a PM (see Figure IX).

In 1973, Laing took out another patent, [07]; this patent described the magnetic gear incorporated into a centrifugal pump. The advantage of using a magnetic gear in a pump is that the two rotating shafts transferred torque without physical contact, thus the pump could be sealed.

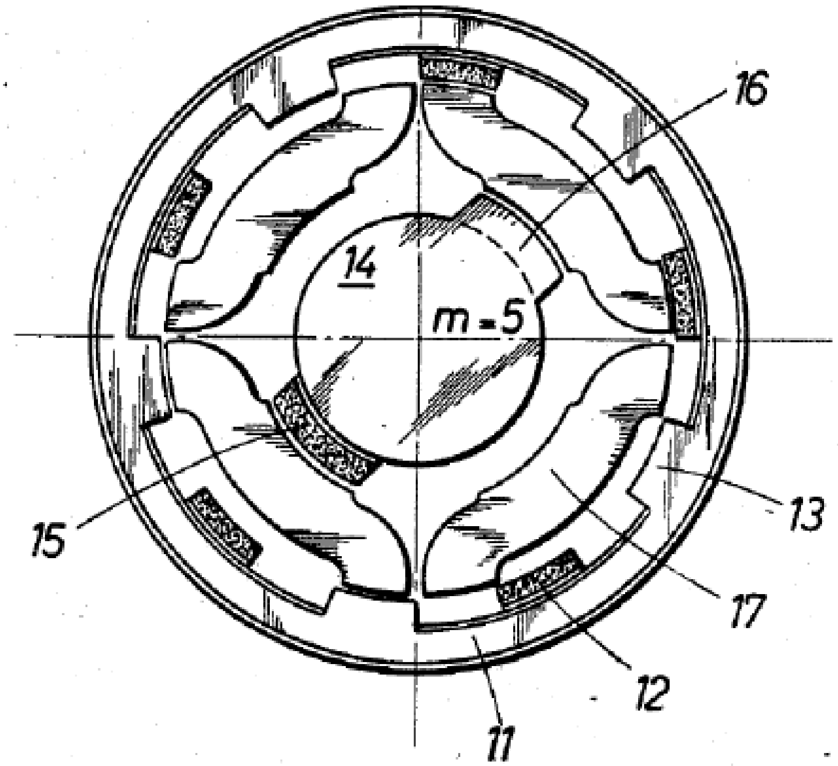

Figure -XXIX-coaxial magnetic gear

Hesmondhalgh et al. (1980) [08] proposed an array of Neuland's [2] magnetic gears (see Figure X), in a hope that the array of gears would increase the maximum torque and efficiency and reduced the cogging torque. However, the total efficiency for the system was very low and the combined gears made the whole system too large and complex.

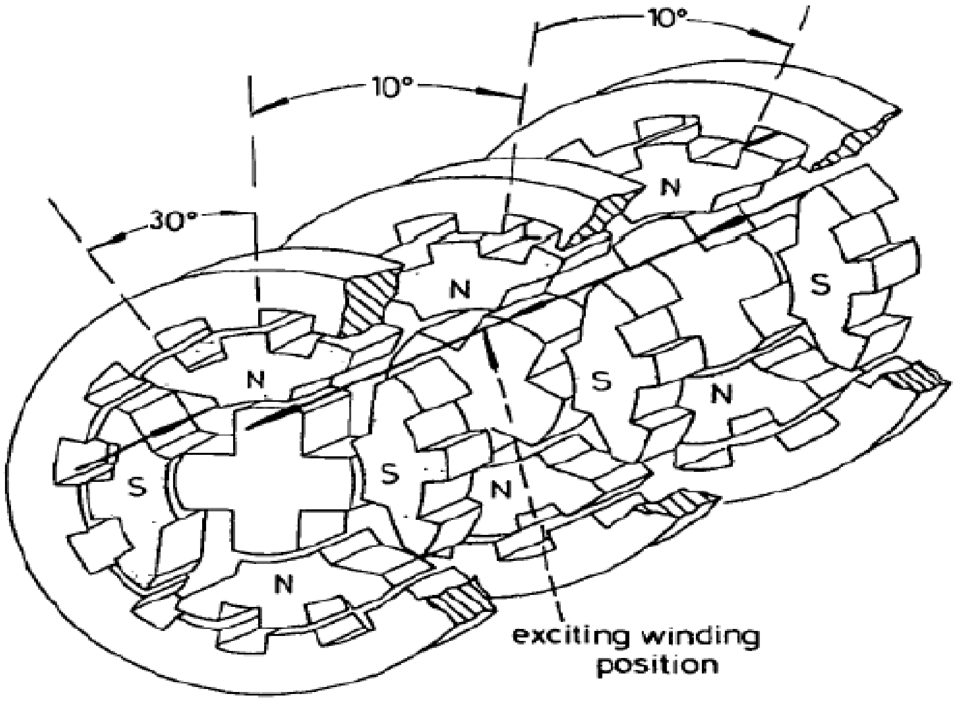

Figure-XXX- A Multi-Element Magnetic Gear

In 1999 Ackerman took out another patent [09] for the same kind of gear, except that the fluxmodulator was moved to the outer rotor (see Figure XIB).

Ackerman et al. [10] received a patent in 1997 for a coaxial magnetic gear. The gear was very similar to the earlier design of 1960[06] except that the flux-modulator was simplified and connected (see Figure XIA). There were three parts which were movable relative to each other. One of the rotors was connected to a drive and one kept stationary, while the remaining one would be the output shaft.

In 1999 Ackerman took out another patent [09] for the same kind of gear, except that the fluxmodulator
was moved to the outer rotor (see Figure XIB).

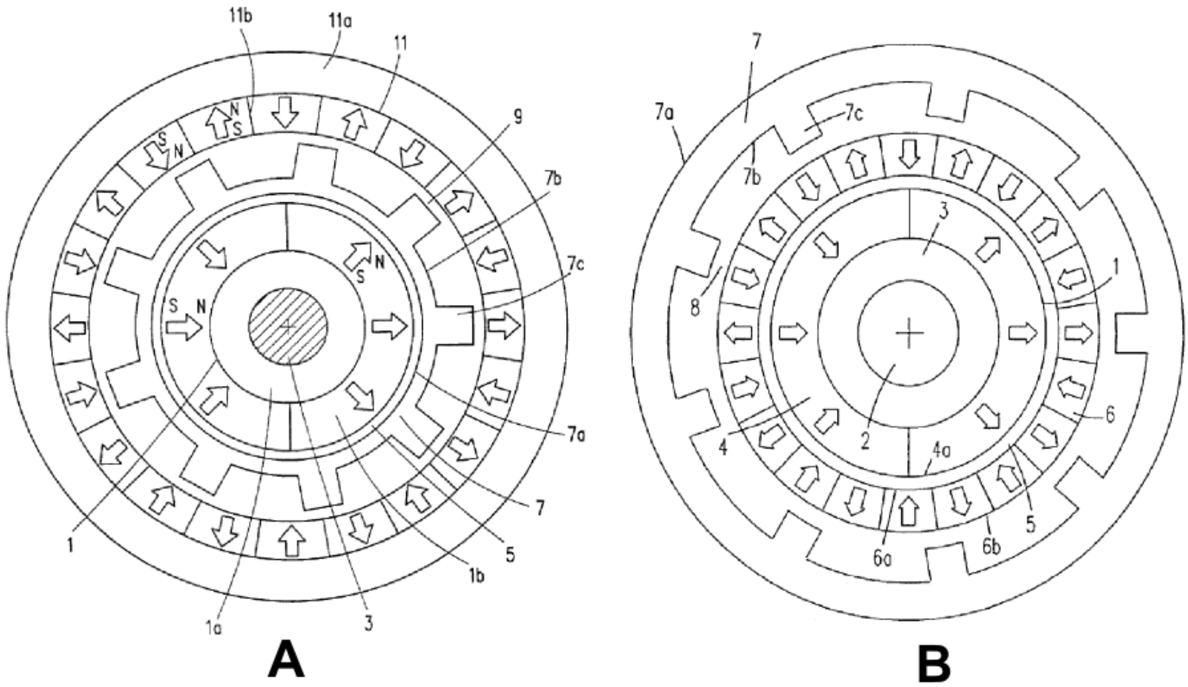

Figure-XXXI-coaxial magnetic gear, A-Middle flux modulator. B-outer flux modulator

Atallah et al. (2000) wrote a paper [12] on a "novel" magnetic gear. The gear was fundamentally the same as Ackerman’s 1997 gear, except that the flux-modulator was not connected (see Figure XII). In the paper the relationship between the number of poles and the number of modulation pieces in the gear were described to determine the gear ratio. It was claimed that by using rare earth magnets a torque density exceeding 100 kNm/m3 could be achieved.

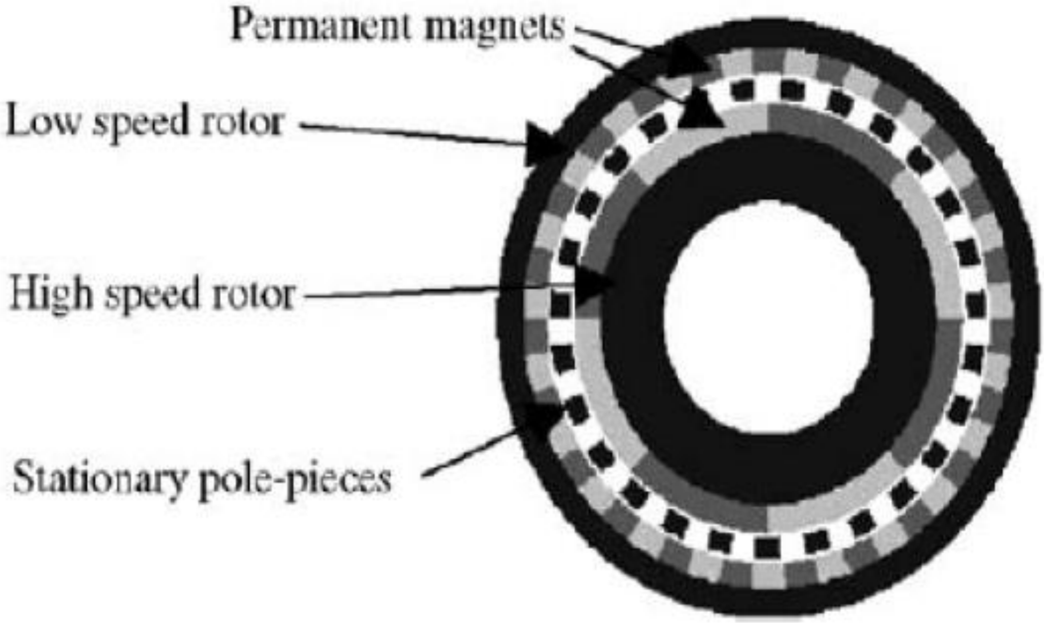

Figure-XXXII- Coaxial Magnetic Gear (Unconnected Modulation Pieces [12]

In 2003 Rasmussen wrote a paper, [13], on a coaxial magnetic gear, the same as described above, except that the inner rotor's magnets were arranged in a spoke-type arrangement and not surface mounted (see Figure XIII). It was calculated that the gear would have a gear ratio of 1:5.5 and a stall torque of 27 Nm. However, the experimental results showed a stall torque of only 16 Nm. The reduction in the stall torque seemed to be caused by the end-effects of the short stack length of the magnets. In the paper MG is also compared with conventional mechanical gears with the same gear ratio and maximum torque capabilities. It was concluded that a theoretical efficiency of 96% could be reached if the end-effect losses were minimized and the gear had a higher torque density when compared to other mechanical gears.

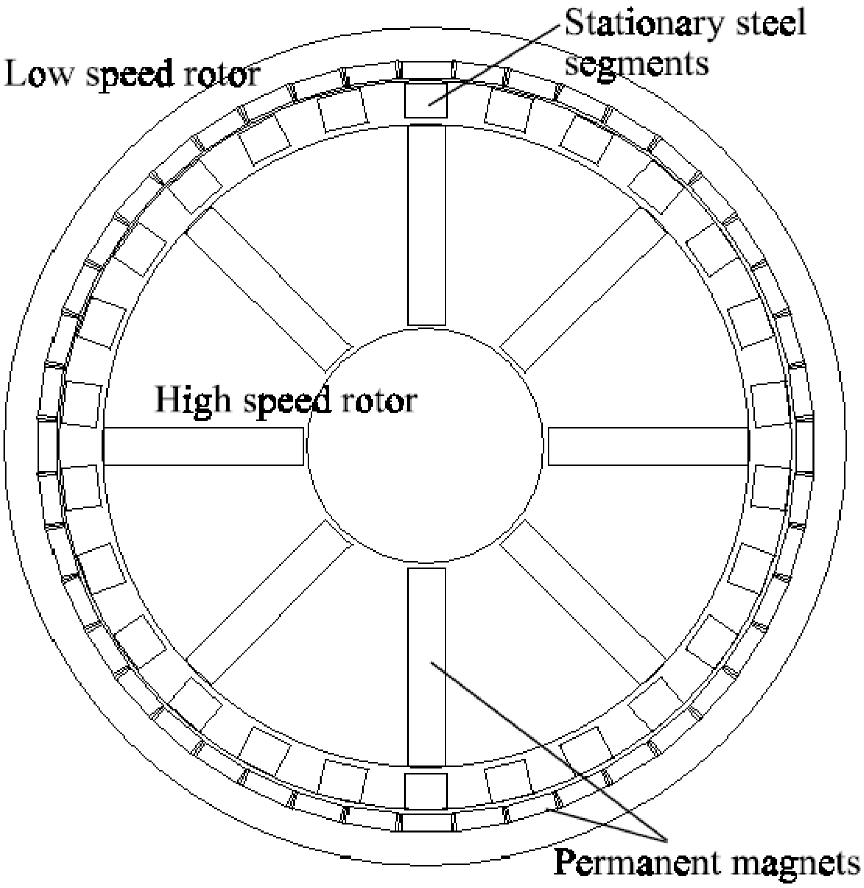

Figure -XXXIII- Coaxial Magnetic Gear with Spoke-Type High Speed Rotor Magnets [13]

Atallah et al. 2005 published a paper [14] on a linear magnetic gear. The gear operated on the same principle as the coaxial magnetic gear. There were three parts that moved relative to each other: two PM armatures connected to steel yokes and one flux-modulator core (see Figure XIV). The flux-modulator core modulated the magnetic flux between the inner and outer PM armatures, so that the PM yokes interacted with the correct number of poles (correct space harmonics). The proposed linear gear was simulated and the results showed that a thrust force of 1.7 MN/m3 could be obtained. It was also shown that a linear magnetic gear combined with a linear electrical machine could obtain a high force density, even with a relatively low gear ratio.

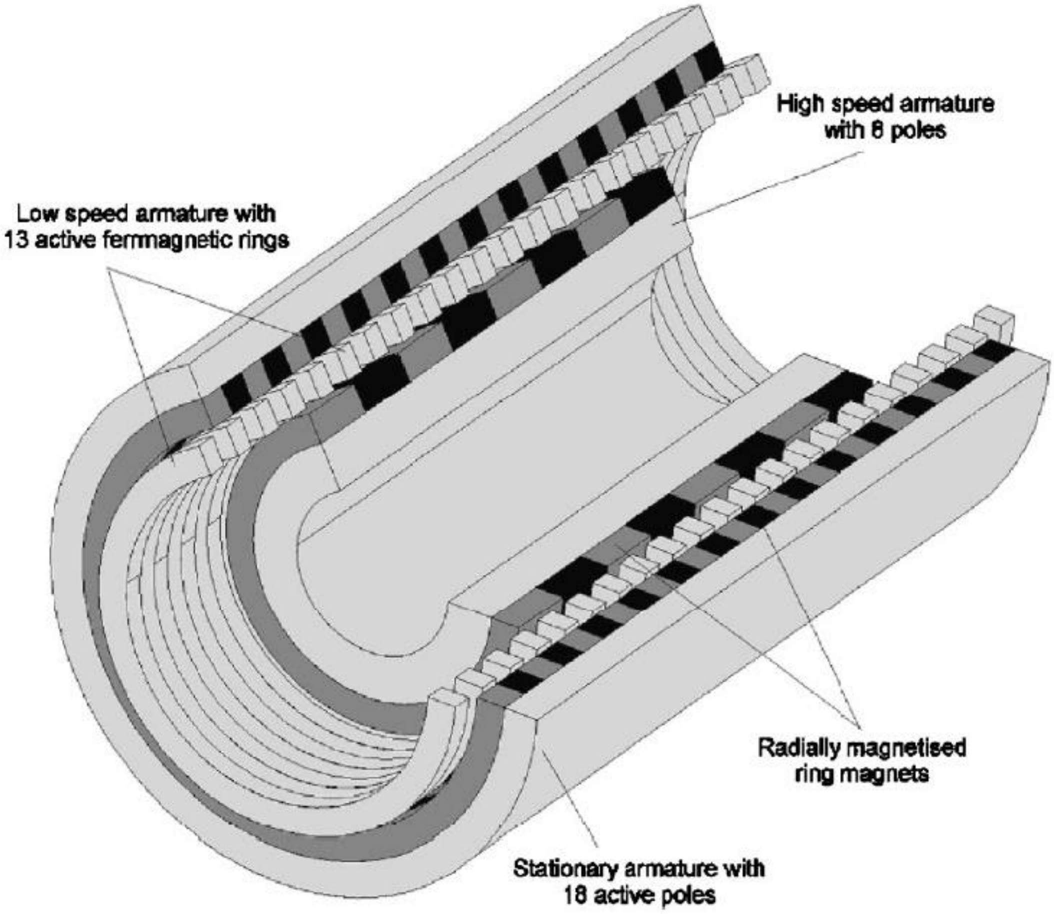

Figure -XXXIV-linear magnetic gear [14]

Rens et al. [15] 2007 proposed a harmonic magnetic gear. The operating principle of the proposed gear was similar to that of a mechanical harmonic gear (see Figure XV). The operating principle of a harmonic gear was that a high-speed input on the wave generator caused gear teeth on the flexible spline (input) to engage with internal teeth on the circular-spline (output). Since the flexible-spline had two teeth less than the circular-spline, each revolution of the input caused a 2-tooth displacement of the output. (Figure XV B shows a magnetic version of the harmonic gear). For the magnetic harmonic gear, the high-speed rotor deformed the flexible low speed rotor, which rotated within the rigid outer stator. The time varying sinusoidal variation of the air gap length modulated the field produced by the magnets on the low speed rotor and resulted in a dominant asynchronous space harmonic field, which interacted with the magnets on the stator to facilitate torque transmission and the magnetic gear action.

The harmonic gearing was further complicated by the need for a low speed rotor assembly with flexible permanent magnets. One way to simplify the design and make it more practical was to use a low speed rigid rotor driven eccentrically by the high-speed rotor so that only a single cyclic variation of the gap occurs between the permanent magnets on the rotor. The rotor at low speed and the stator (see Figure XVI). This version was much better than the flexible version (as can be seen in XV B) but not without complexities.

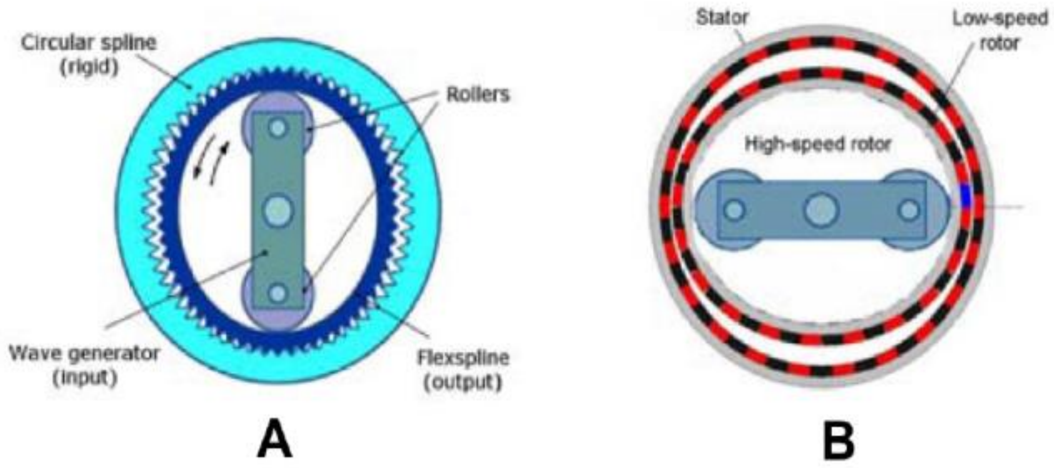

Figure -XXXV- A-Mechanical Harmonic Gear. B-Magnetic Harmonic Gear [15]

The problem with this design is that the low speed rigid rotor has turned eccentrically; the output shaft had to be connected to this rigid rotor at low eccentric speed and this could only be done with a flexible coupling or with two bearings in one another but with the same eccentric distance. (Figure XVI shows cycloidal bearings with eccentric distance between bearings). Another problem associated with the eccentric distance is that an unbalanced magnetic force has been generated because one side of the high speed rotor was always closer to the low speed rotor (the variable air gap).

Figure -XXXVI- More Practical Harmonic Magnetic Gear

In 2007 Atallah et al. [16], patented a MG integrated into a brushless PM machine, which they called a PSEUDO machine. In the same year Atallah were granted another international patent, [17], for a harmonic magnetic gear, similar to the one described in a previous paper [15]. In 2008, he wrote two more papers about the PSEUDO drives, [18] [19]. In both papers the operating principle of magnetically geared brushless machines were described. In both papers, it was concluded that the machines could reach torque densities in excess of 60 kNm/m3 and that the machines had a power factor of 0.9 or higher.

In 2011 Jiabin Wang, Kais Atallah, and S. D. Carvley describe [20] a continuously variable transmission device, in which torque transmission and variable gear ratio is achieved by magnetic means. It consists of a stator, which accommodates a 3-phase winding, and three concentric rotors: control rotor, input and output rotors. The control rotor has Pc number of pole-pairs on the outer surfaces and Pl number of pole-pairs of permanent magnets on its inner surface. The magnets on the outer surface of the control rotor interact with the currents in the 3-phase stator winding to produce torque in the same way as conventional brushless permanent magnet (PM) machines. The magnets on the inner surface of the control rotor interact with the input and output rotors to produce magnetic gearing action. It has been shown that by controlling the speed of the control rotor, the gear ratio between the output rotor and input rotor can be varied.(see figure XVII and XVIII)

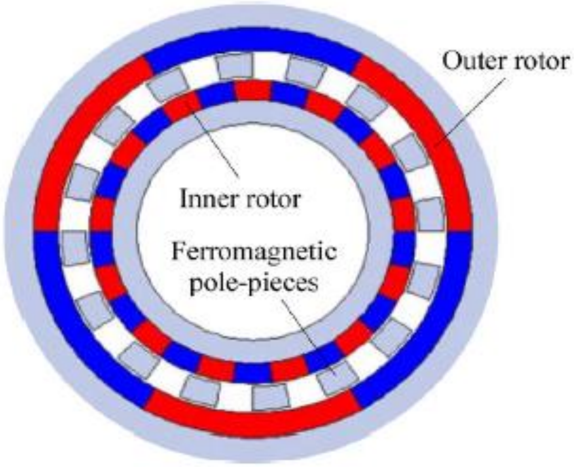

Figure-XXXVII-schematic of magnetic gear [20]

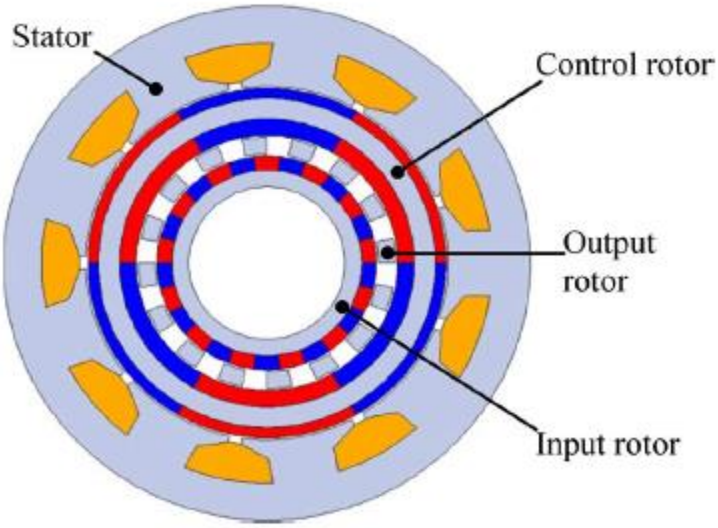

Figure -XXXVIII- Schematic of magnetic continuously variable transmission [20]

II- Definition of a magnetic coupling

A magnetic coupling is a coupling that transfers the torque of a tree, but using a magnetic field rather than a mechanical physical connection.

Magnetic shaft couplings are most often used for liquid pumps and propeller systems because a static physical barrier can be placed between the two trees to separate the fluid from the engine operating in the air. Magnetic shaft couplings prevent the use of shaft seals, which eventually wear out and can not be slide between two surfaces against each other. Magnetic couplings are also used to facilitate the maintenance of systems that generally require alignment precision when physical shaft couplings are used, as they allow greater axis error between the motor and the driven shaft. [21]

III- Magnetically geared machines

Gears can generally be used to increase the total system torque density of a drive train compared with a direct-drive solution, at the cost of additional complexity. Magnetic gears are not different from mechanical gears in this context. However, several interesting possibilities exist by which a magnetic gear can be integrated with an electrical machine into a single compact unit. In this way, the torque density can be raised beyond what can be achieved with a cascaded configuration.

This type of integration is illustrated in Fig.XIX. The flux-modulated magnetic gear is especially suited to this kind of integration due to its simple and balanced design.

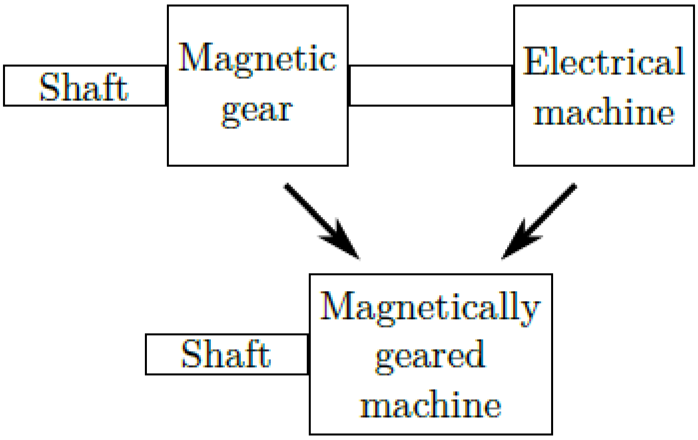

Figure-XXXIX-magnetically geared machine

A list of published prototypes with their outer diameter (Do), gear ratio (Gr) and active volume torque density (T=VA) is given in Table 01. Note that the torque densities reported are not directly comparable, since different types of torque are used in the calculations. However, it is clear that the torque densities achieved by these machines are generally very high.

Description	D_o [mm]	G_r	T/V_A [kNm/m^3]
Atallah et al.	178	11.5	>60 (measured continuous)
Jian et al. Jiam et al.	194	7.3	87 (simulated stall)
Rasmussen	268.5	8.83	92 (measured stall)
Wang et al.	320	6.6	105 (simulated stall, gear only)

Table -I- List of published prototypes

IV- Magnetic gear applications

Due to the many advantages that we offer magnetic couplings, we will find them everywhere in industrial applications such as the sectors of: energies renewable; maritime, petrochemical ... etc. as show in the following examples:

IV-1 wind turbines

The goal will be to change the mechanical couplings currently used in wind turbines by magnetic couplings is part of the objectives of manufacturers.

Like the study proposed by [OJS12] this work was supervised by ERDF under the title "Wind and Hydrogen Based Autonomous Energy Suply System" with the aim of finding the parameters of construction of this coupling in order to transmit a torque of 250Nm which is the nominal torque of the permanent magnet synchronous generator uses. This coupling is radial flow based on NdFeB magnet with an axial length of 185 mm and an external diameter of 121.7 mm.

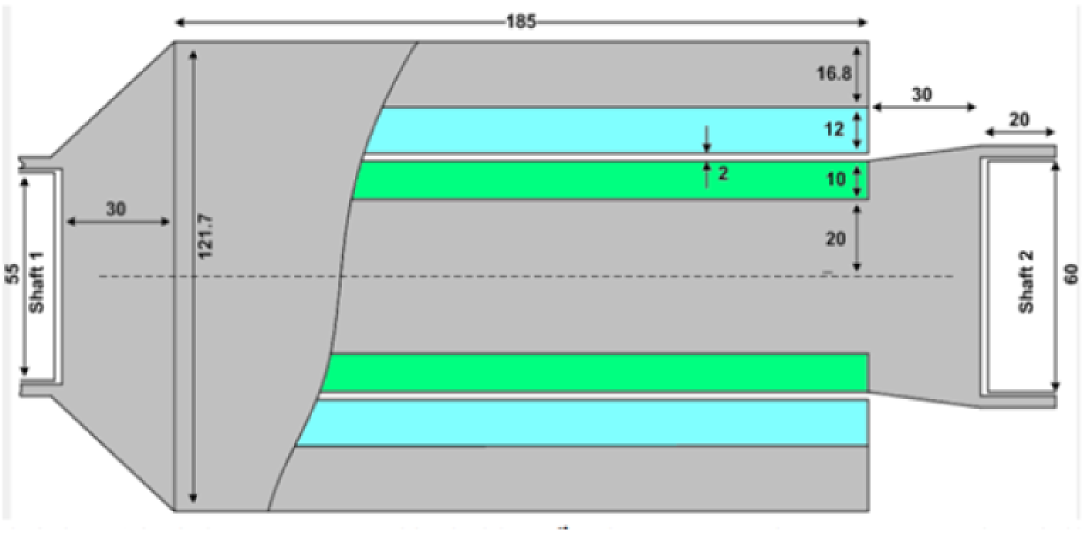

Figure -XL- Magnetic coupling for use in wind farms

IV-2 Hybrid vehicles

With the dwindling of fossil fuel reserves the world switched to electric vehicles but still using mechanical couplings as for cars to traction, which are the most accessible, therefore which opens to more possibility of research. Among the possibilities available to us for the transmission of the movement, we have:

- **Transmotor**

The transmotor is an electric machine composed of a stator connected to the motor and a rotor connected to the transmission shaft. The stator receives the speed of the motor and it has itself an electric port, so when a current is sent to the stator it will generate an induced EMF variation that will be picked up by the rotor with permanent magnets so the rotor will follow the rotating stator field.

The study was conducted to find hybrid electric vehicle (HEV) trains that could benefit from new types of gears. The transmotor, presented as an electromagnetic machine, has been studied by looking at all the different modes of operation.

Nine distinct modes of operation were found; representing instances where the stator and rotor were either free to move or blocked in one position. The power at the electric port was found by a speed summation in (I.01). The torque of the machine has been found to be just a 1: 1 coupling, as shown (I.02);

$$Pelec = Tr(\omega r + \omega s) \qquad \text{(I.01)}$$

$$|Tr| = |Ts| \qquad \text{(I.02)}$$

As previously stated, each of the nine distinct modes of operation was falling in one of the four categories of operation of an electric machine, except in the case where the rotor and the stator were rotating at the same speed, in which case the machine functions simply as an electromagnetic lock. It has been assumed that the structure of the electric machine is that of a variable reluctance machine (MRV) or a DC machine (MCC) for the operating mode in which the rotor is blocked.

However, in the case where $\omega r = \omega s$, only the MRV is able to function in this mode in steady state.

The role of the internal combustion engine (ICM) is to generate power that will be stored in the batteries. This energy is used to power the electric traction of the vehicle.

The role of the internal combustion engine (ICM) is to generate power that will be stored in the batteries. This energy is used to power the electric traction of the vehicle.

There is another mode where the MCI and the electric can connect at the same time to the mechanical box for their couples to add.

- **Magnetic transmission**

Among the innovations of the 21st century is to couple a magnetic box to a vehicle, and among them the coupling between a hybrid electric vehicle (EVH) and a magnetic box.

The idea of this mating is similar to the systems already proposed before. This system is composed of electromechanical elements connected directly to the driving wheels, or through elements connected in series towards the wheels.

According to [22] and [24] [25] the dimensions of this type of coupling are identical to an MSAP to be considered with the vehicle itself. The electromechanical gearbox that does not depend on the other elements so that one could place it inside the wheel herself. This type of assembly is shown in Figure XXI.a where the outer rotor is connected directly to the wheel axis. Figure XXI.b shows the possibility of connecting the magnetic gear inside the drive shaft before reaching the differential.

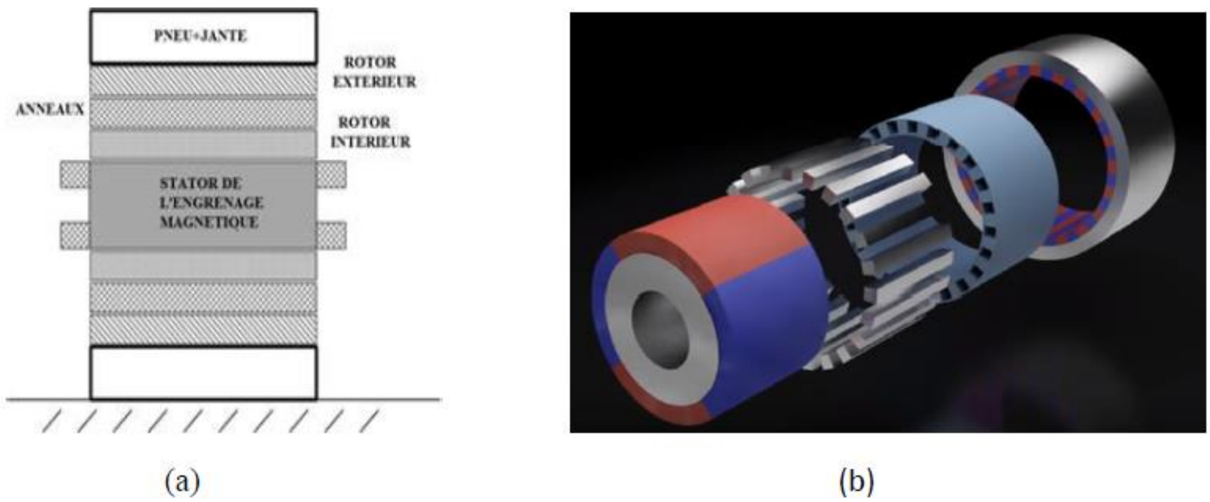

Figure-XLI- Magnetic gear, (a) Gear in the axis of the wheel. (b) sets of basic elements

- **Magnetic levitation train**

- The Magnetic levitation train (French MAGLEV) is an experimental train that has been tested in Japan since 1990. A 19 km line was built in Yamanashi for these tests. Since April 3, 1997, tests are regularly carried out and on April 14, 1999, the Maglev reached a speed of 552 km / h and currently reaches 603km / h.
- The Transrapid is a German project to connect Munich Airport to the city with a magnetic levitation train. The only existing and functional Transrapid is now in China in Shanghai. It has been in service since 2002 and connects the airport and the city. The line was to be longer, but following the protests of local residents, who feared nuisance due to possible magnetic radiation.

V- Advantages

The possible applications for magnetic gears and magnetically geared machines are numerous. Magnetic gears can replace mechanical gears in many applications due to the following advantages they hold:

- **Frictionless torque transfer** : Torque is transferred via magnetic forces, which means that magnetic gears do not suffer from wear and losses associated with meshing teeth.
- **Low maintenance** : The only parts in a magnetic gear which require lubrication are the bearings, for which the maintenance requirements are typically very low.
- **Overload protection** : Magnetic gears slip when their pull-out torque is exceeded, while mechanical gears may be damaged under overload conditions. This mechanism can also be used to protect other components in the drive train.
- **Reduced noise** : Magnetic gears are expected to be low-noise devices, due to smooth torque transfer characteristics and absence of tooth contact.
- **High-efficiency** : The mechanisms of power loss in magnetic gears are very different from those in mechanical gears. Magnetic gears can also achieve high efficiencies.

Chapter 02

A magnetic continuously variable transmission

I- Introduction

I-1 continuously variable transmission (**CVT**), also known as a **shiftless transmission**, single-speed transmission, stepless transmission, pulley transmission, or, in case of motorcycles, a 'twist-and-go', is an automatic transmission that can change seamlessly through a continuous range of effective gear ratios. This contrasts with other mechanical transmissions that offer a fixed number of gear ratios. The flexibility of a CVT with suitable control may allow the input shaft to maintain a constantangular velocity even as the output speed varies.

A belt-driven design offers approximately 88% efficiency, which, while lower than that of a manual transmission, can be offset by lower production cost and by enabling the engine to run at its most efficient speed for a range of output speeds. When power is more important than economy, the ratio of the CVT can be changed to allow the engine to turn at the RPM at which it produces greatest power. This is typically higher than the RPM that achieves peak efficiency. In low-mass low-torque applications (such as motor scooters) a belt-driven CVT also offers ease of use and mechanical simplicity [26]

I-2 A magnetic continuous variable transmission system was developed at the University of Sheffield in 2006 and later commercialized. *m*CVT is a variable magnetic transmission which gives an electrically controllable gear ratio. It can act as a power split device and can match a fixed input speed from a prime mover to a variable load by importing/exporting electrical power through a variator path. The *m*CVT is of particular interest as a highly efficient power-split device for blended parallel hybrid vehicles, but also has potential applications in renewable energy, marine propulsion and industrial drive sectors. [26]

II- presentation of the study model

Our model of study will be based on the model [20]. This device can be used to replace the mechanical counterpart of the CVT system to improve the efficiency and reliability of the transmission.

The magnetic gear has many advantages in terms of efficiency, reliability, reduced maintenance, inherent protection against overloads, etc. It has been shown that magnetic gears that use rare earth magnets can reach over 100 kNm/m^3.

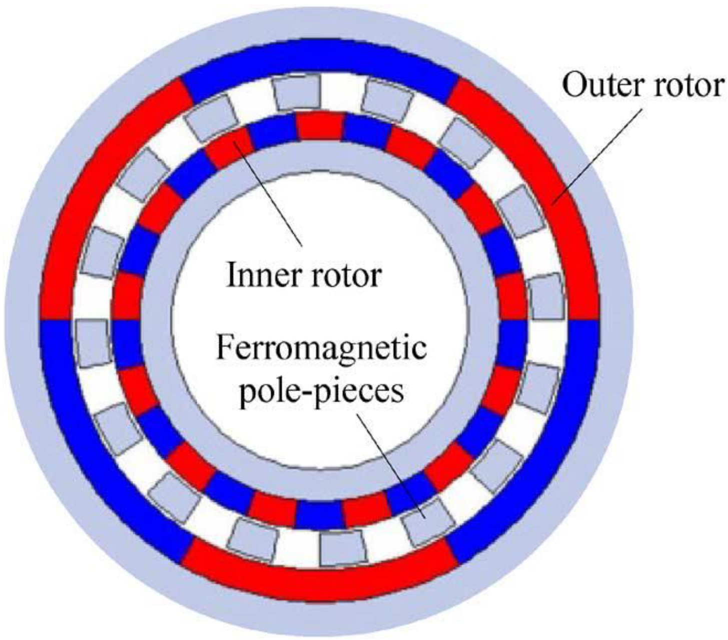

Figure schematic of magnetic gear- XXII

The magnetic gear shown in Figure XXII consists of three concentric rotors. The inner and outer rotors are equipped with permanent magnet arrays whilst the intermediate rotor carries a number of ferromagnetic pole-pieces. When one of the rotors is anchored to a stationary frame, the remaining two rotors form a magnetic gear with a fixed gear ratio. Based on this magnetic gearing principle, a continuously variable transmission device, as shown Figure XXIII, is proposed, in which torque transmission and variable gear ratio is achieved by magnetic means [27]. It consists of a stator, which accommodates a 3-phase winding, and three concentric rotors: the control rotor and the input and output rotors. The control rotor has number of pole-pairs of permanent magnets on its inner surface and number of pole-pairs on the outer surfaces. The magnets on the outer surface of the control rotor interact with the currents in the 3-phase stator winding to produce torque in the same way as conventional brushless permanent magnet (PM) machines. The input rotor is located innermost and has number of pole-pairs of magnets whiles the output rotor is in the middle and comprises of number of ferromagnetic pole-pieces. The interaction of the magnetic field due to the magnets on the inner surface of the control rotor with the magnetic field which results from the magnets on the input rotor and modulated by the ferromagnetic pole-pieces produces magnetic gear action [28] – [29]. By controlling the speed of the control rotor, the gear ratio between the output rotor and input rotor can be varied. Design studies and numerical analysis of magnetic CVT performance have been reported in [30].

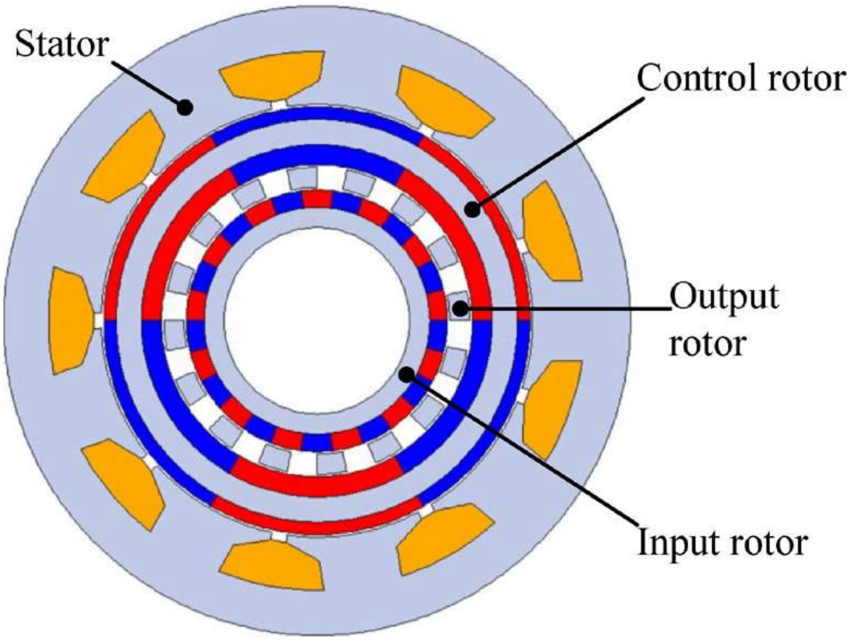

Figure – XXIII- schematic of a magnetic continuously variable transmission

III- Principle of operation of Magnetic Gearing

Fundamental to the operation of a coaxial magnetic gear are the magnetic fields produced by the permanent magnets on either the high- or low-speed rotors by the steel pole pieces (flux-modulation pieces), which result in space harmonics having the same number of poles as the related magnet rotor.

In Figure XXIV a generic layout of a radial field magnetic gear is presented. The flux distribution in radial direction at a radial distance r and angle *q* produced by either permanent magnet rotor, without taking into consideration the flux-modulator, can be written in the following form [29] :

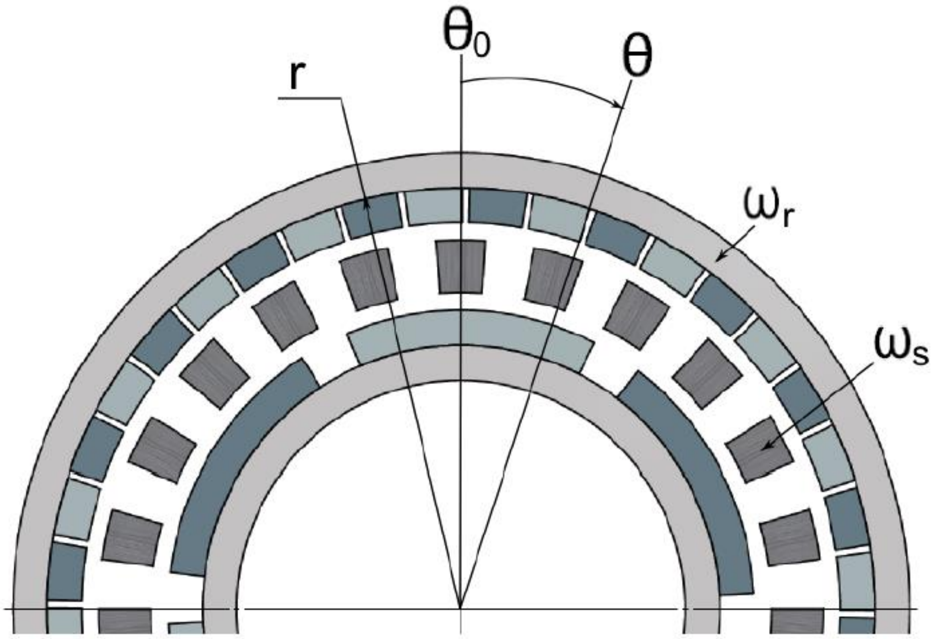

Figure – XXIV- Magnetic Gearing Parameters

$$\boldsymbol{B_{rA}(r,\theta) = \left\{\sum_{m=1,3,5,\ldots} b_{rm}(r)\cos(mP(\theta-\omega_r t)+mP\theta_0)\right\}} \qquad \textbf{\textit{(02.01)}}$$

And the modulation function can be written as

$$\boldsymbol{B_{rB} = \left\{\lambda_{r0}(r) + \sum_{j=1,2,3,\ldots} \lambda_{rj}(r)\cos\left(jN_s(\theta-\omega_s t)\right)\right\}} \qquad \textbf{(02.02)}$$

The resultant field components for the radial component are

$$B_r(r,\theta) = B_{rA}(r,\theta) \times B_{rB}(r,\theta) \qquad \textbf{\textit{(02.03)}}$$

Similary for the circunferential flux distribution, we have

$$\boldsymbol{B_{\theta A}(r,\theta) = \left\{\sum_{m=1,3,5,\ldots} b_{\theta m}(r)\sin(mP(\theta-\omega_r t)+mP\theta_0)\right\}} \qquad \textbf{(02.04)}$$

$$\boldsymbol{B_{\theta B} = \left\{\lambda_{\theta 0}(r) + \sum_{j=1,2,3,\ldots} \lambda_{\theta j}(r)\cos\left(jN_s(\theta-\omega_s t)\right)\right\}} \qquad \textbf{(02.05)}$$

$$B_\theta(r,\theta) = B_{\theta A}(r,\theta) \times B_{\theta B}(r,\theta) \qquad \textbf{\textit{(02.06)}}$$

Where $\boldsymbol{P}$ is the number of pole-pairs on a permanent magnet rotor, N_s is the number of modulation pieces, ω_r is the rotational velocity of the permanent magnet rotor and ω_s is the rotational velocity of the flux-modulator. The Fourier coefficients for the radial and circumferential flux density distribution without the flux-modulation pieces are B_{rm} and$B_{\theta m}$, respectively. The Fourier coefficients for the radial and circumferential components of the flux density distribution resulting from the introduction of the flux-modulation pieces are λ_{rj} and $\lambda_{\theta j}$, respectively

On substitution of (02.01) and (02.02), Equation (02.03) can be further expressed as:

$$\boldsymbol{B_r(r,\theta)=\lambda_{r0}(r)\times\sum_{m=1,3,5,\ldots} b_{rm}(r)\cos\{(mP(\theta-\omega_r t)+mP\theta_0)\} + \frac{1}{2}\sum_{m=1,3,5,\ldots}\sum_{j=1,2,3,\ldots} b_{rm}(r)\lambda_{rj}(r)\cos\left\{(mP+jN_s)\left(\theta-\frac{mP\omega_r+jN_s\omega_s}{mP+jN_s}t\right)+mP\theta_0\right\} + \frac{1}{2}\sum_{m=1,3,5,\ldots}\sum_{j=1,2,3,\ldots} b_{rm}(r)\lambda_{rj}(r)\cos\left\{(mP-jN_s)\left(\theta-\frac{mP\omega_r-jN_s\omega_s}{mP-jN_s}t\right)+mP\theta_0\right\}}$$

(02.07)

Similarly, on substitution of Equation (02.04) and (02.05), Equation (02.06) becomes

$$B_{\Theta}(r,\Theta)=\lambda_{\Theta 0}(r)\times\sum_{m=1,3,5,\ldots} b_{\Theta m}(r)\sin\{(mP(\Theta-\omega_r t)+mP\Theta_0)\}+\frac{1}{2}\sum_{m=1,3,5,\ldots}\sum_{j=1,2,3,\ldots} b_{\Theta m}(r)\lambda_{\Theta j}(r)\sin\left\{(mP+jN_s)\left(\Theta-\frac{mP\omega_r+jN_s\omega_s}{mP+jN_s}t\right)+mP\Theta_0\right\}-\frac{1}{2}\sum_{m=1,3,5,\ldots}\sum_{j=1,2,3,\ldots} b_{\Theta m}(r)\lambda_{\Theta j}(r)\sin\left\{(mP-jN_s)\left(\Theta-\frac{mP\omega_r-jN_s\omega_s}{mP-jN_s}t\right)+mP\Theta_0\right\}$$

(02.08)

From Equation (02.07) and (02.08), it can be seen that the number of pole pairs in the space harmonic flux density distribution produced by either the high- or low-speed rotor is given by

$$P_{m,k}=|mP_1+kN_s| \qquad (02.09)$$

$$m=1,3,5,\ldots,\infty$$

$$k=0,\pm1,\pm2,\pm\cdots,\pm\infty$$

The rotational velocity of the flux density space harmonic is given by

$$\omega_{m,k}=\frac{mP}{mP+kN_s}\omega_r+\frac{kN_s}{mP+kN_s}\omega_s \qquad (02.10)$$

$$m=1,3,5,\ldots,\infty$$

$$k=0,\pm1,\pm2,\pm\cdots,\pm\infty$$

From Equation (2.10), it can be seen that the velocity of the space harmonics due to the introduction of the flux-modulator ($k\neq 0$), is different to the velocity of the rotor which carries the permanent magnets. Therefore, in order to transmit torque at a different speed (change the gear ratio), the number of pole-pairs of the other permanent magnet rotor must be equal to the number of pole-pairs of a space harmonic for which ($k\neq 0$). Since the combination $m=1$ and $k=-1$ results in the highest asynchronous space harmonic, the number of pole-pairs of the other rotor must be equal to (N_s-P). The gear ratio when the flux-modulator is held stationary ($\omega_s=0$), is then given by

$$G_r = \frac{N_s - P_H}{P_H} \quad (02.11)$$

Or

$$G_r = \frac{P_L}{P_H} \quad (02.12)$$

Which gives

$$N_s = P_H + P_L \quad (02.13)$$

Where P_H and P_L are the number of pole-pairs on the high- and low-speed rotors, respectively. Sometimes, it may be preferred to keep the outer rotor stationary ($\omega_r = 0$) as it may simplify the overall mechanical design. The torque will then be transmitted to the flux-modulator instead of the outer rotor, the gear ratio then becomes

$$G_r = \frac{N_s}{P_H} \quad (02.14)$$

IV- Principle of operation of Magnetic CVT

Without loss of generality, Figure XXV shows the angular displacements of three rotors with respect to the stationary reference, which is used to define angular displacements of the three rotors.

For the purpose of discussion, their equivalent current sheets represent the permanent magnets on the inner surface of the control rotor. The fundamental component of the radial flux density produced by permanent magnets on the input (inner) rotor is modulated by the fundamental component of the permeance function of ferromagnetic pole-pieces of the output rotor, and the resulting flux density at an angle θ and a radial distance r is given by [20]

$$B_h(r,\theta) = B_{h1}(r)\cos[P_h(\theta-\theta_h)] \times [\lambda_1(r)\cos(N_s(\theta-\theta_s))] \quad 03.01$$

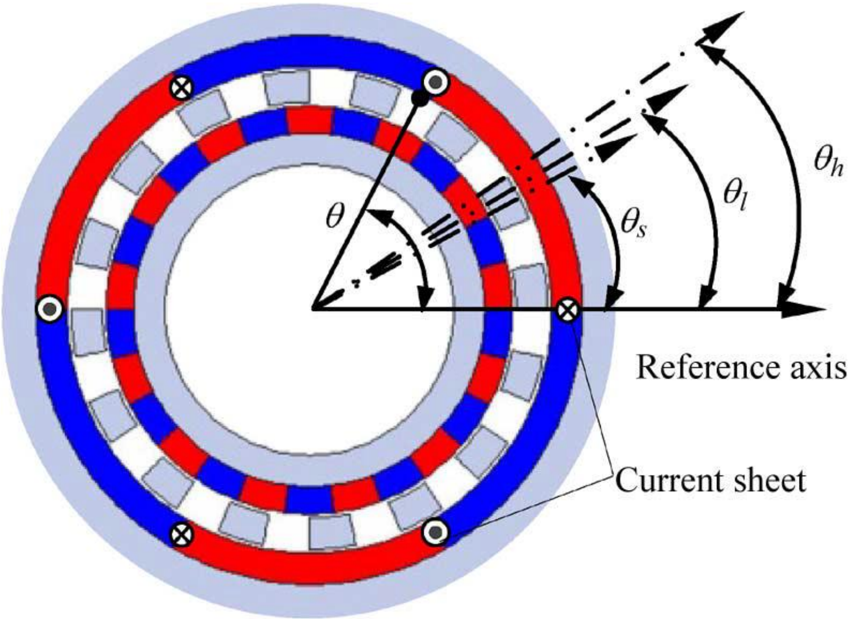

Figure ***Erreur ! Il n'y a pas de texte répondant à ce style dans ce document.*** *XXV*- Reference frame and angular displacement of three rotors

Where B_{h1} and λ_{h1} are Fourier coefficients of the fundamental components of the flux density due to the magnets on the input rotor and the permeance function of the output rotor, respectively.

Both are a function of r. θ_h And θ_s represent the angular displacement of the input and output rotors, respectively. The reference axis of the input rotor is fixed to the centre of an N pole whilst the reference of the output rotor coincides with centre of a ferromagnetic pole piece, as shown in Figure XXV. From trigonometric identity, (03.01) may be expressed as

$$B_h(r,\theta) = \frac{\lambda_1(r)\, B_{h1}(r)}{2}\cos[(P_h + n_s)\theta - n_s\theta_s - P_h\theta_h] + \frac{\lambda_1(r)\, B_{h1}(r)}{2}\cos[(n_s - P_h)\theta - n_s\theta_s - P_h\theta_h] \qquad 03.02$$

The magnets on inner surface of the control rotor can be represented by the current sheets distributed on both sides of the magnets, as shown in Figure XXV, and the equivalent surface current density, J_c is given

$$J_c = \frac{B_{rem}}{\mu_0\mu_r} \qquad 03.03$$

Where B_{rem} and μ_r are the remanence and relative recoil permeability of the magnets, respectively, and μ_0 is the permeability in free space. The torque acting on the control rotor because of the interaction of the magnetic field produced by the magnets on the input rotor and the equivalent current sheets on the control rotor can be obtained by

$$T_{lem} = \int_s (J_c \times B) \times \vec{r} ds \qquad 03.04$$

Where S is the surface area of the current sheets. Since J_c has only z component and $ds = I_a\, dr$, where I_a is the axial length of the device, (03.04) can be simplified and the torque acting on $2P_l$ poles of the magnets can be evaluated by

$$T_{lem} = -T_m \sum_{j=1,2\ldots}^{2P_l} (-1)^{j-1} \times \sin\left[(P_h + n_s)\theta_l - n_s\theta_s - P_h\theta_h + \frac{P_h + n_s}{P_l}\pi(j-1)\right] - T_m \sum_{j=1,2\ldots}^{2P_l} (-1)^{j-1} \times \sin\left[(n_s - P_h)\theta_l - n_s\theta_s - P_h\theta_h + \frac{n_s - P_h}{P_l}\pi(j-1)\right] \qquad 03.05$$

Where θ_l is the angular displacement of the control rotor with respect to the reference axis, as shown in Figure XXV. T_m is given

$$T_m = I_a J_c \sin\left(\frac{P_l \alpha_p}{2}\right) \int_{Rc_1}^{Rc_2} \lambda_1(r) B_{h1}(r) rdr \qquad 03.06$$

Where α_p is the pole-arc angle of the magnets on the inner surface of the control rotor, and Rc_1 and Rc_2 are the inner and outer radii of the magnets. As can be seen from the summation terms in (03.05), they becomes non zero only if $P_l = (n_s + P_h)$ or $P_l = (n_s - P_h)$.By way of example, let $P_l = (n_s - P_h)$, the resultant electromagnetic torque acting on the control rotor is given by (03.07)

$$T_{lem} = -T_{max} \sin(P_l \theta_l + P_h \theta_h - n_s \theta_s) \qquad 03.07$$

Where the magnitude of torque,T_{max}, is given by

$$2 P_l T_m \qquad 03.08$$

T_{max} is dependent on the geometric parameters of the three rotors and the properties of the magnets and ferromagnetic materials. The negative sign in (7) indicates the direction of the torque is opposite to the referred load angle.$\theta_e = P_l \theta_l + P_h \theta_h - n_s \theta_s$ In steady state, the referred load angle must be constant, which leads to

$$\frac{d(P_l \theta_l + P_h \theta_h - n_s \theta_s)}{dt} = 0 \; or \; (P_l \Omega_l + P_h \Omega_h - n_s \Omega_s) = 0 \qquad 03.09$$

Where Ω_l, Ω_h and Ω_s are the mechanical angular speed of rotation of the control rotor, the input rotor and the output rotor. The gear ratio between the output and the input rotors is, therefore, given by

$$G_r(\Omega_l) = \frac{\Omega_s}{\Omega_h} + \frac{P_l \Omega_l}{n_s \Omega_h} \qquad 03.10$$

Thus, by controlling the speed, Ω_l of the control rotor in relation to the input rotor speed, Ω_h , the gear ratio between the input and output rotors can be adjusted.

The torques, T_{hem} and T_{sem} , acting on the input and output rotors, respectively, can be derived by assuming that the system is lossless. Hence, the following equations are satisfied

$$T_{lem} + T_{hem} + T_{sem} = 0 \qquad 03.11$$

$$\Omega_l T_{lem} + \Omega_h T_{hem} + \Omega_s T_{sem} = 0 \qquad 03.12$$

Eliminating T_{hem} from (03.11) and (03.12) yields

$$T_{lem} = -\frac{1-\frac{\Omega_s}{\Omega_h}}{1-\frac{\Omega_l}{\Omega_h}} T_{sem} \qquad 03.13$$

Substituting (03.10) into (03.13) and noting that $P_l = (n_s - P_h)$ results in

$$T_{sem} = \frac{n_s}{P_l} T_{max} \sin(P_l\theta_l + P_h\theta_h - n_s\theta_s) \qquad 03.14$$

Consequently from (03.11), T_{hem} is obtained as

$$T_{hem} = -\frac{P_h}{P_l} T_{max} \sin(P_l\theta_l + P_h\theta_h - n_s\theta_s) \qquad 03.15$$

If the external torques applied to the control, input and outputvrotors are denoted by T_l, T_h and T_s, respectively, and friction and windage torques are neglected, the equation of motion governing the mechanical dynamics of the CVT is given by

$$J_h \frac{d^2\theta_h}{dt^2} = T_h - \frac{P_h}{P_l} T_{max} \sin(P_l\theta_l + P_h\theta_h - n_s\theta_s)$$

$$J_l \frac{d^2\theta_l}{dt^2} = T_l - T_{max} \sin(P_l\theta_l + P_h\theta_h - n_s\theta_s)$$

$$J_s \frac{d^2\theta_s}{dt^2} = T_s - \frac{n_s}{P_l} T_{max} \sin(P_l\theta_l + P_h\theta_h - n_s\theta_s) \qquad 03.16$$

V- Conclusion

In this chapter, we have presented a magnetic continuously variable transmission, its operating principle and the equations governing this gear based on the [20] model.

We have shown that by integrating a magnetic gear with a brushless PM machine, a continuously variable transmission device can be realized. Compared with other CVTs reported to date, the magnetic CVT has a number of advantages in terms of efficiency, reliability, reduced maintenance and inherent overload protection, etc.

Chapter 03

Finite Element Analysis

I- Introduction

Given the complexity of the system to be studied, we have opted for an analysis by the method of finite elements using the FEMM software. The construction of the magnetic transmission system will be done using the so-called LUA programming language.

LUA will allow us to introduce specific forms of our structure and give instructions, to which FEMM software will allow us to calculate magnetic induction and torque.

I-1 Software description

Finite Element Method Magnetics (FEMM) is a two-dimensional (2D) Cartesian and two-dimensional axisymmetric software, dedicated to solving electrostatic and electromagnetic problems in the low frequency domain, using the finite element method. Its user-friendly nature and interesting performance make it an attractive tool for Computer Aided Design of electro-technical devices. It consists of three main parts. [31]

I-2 The preprocessor

Allows, using techniques from Computer Aided Design (CAD), to describe the geometry of the domain, its physical properties and its boundary conditions and to mesh automatically or manually with program assistance.

The plot of a given geometry is done by introducing points whose coordinates are entered at the keyboard and this happens after having defined the field of study, then we define lines (which can be segments of lines or arcs of curves) and regions are described as domain parts delimited by these lines.

Each region is assigned a material extracted from a library of materials of which has the software or introduced, and the size of the associated mesh. Next, define the schema or data of the sources (current, current density), the boundary conditions on the specific boundaries of the field of study. The domain thus obtained, consisting of a certain number of different media, is discretized into small elements by a triangular mesh; each triangle being spotted by its three vertices. In each element, the vector potential is approximated by a polynomial of the first degree.

I-3 the solver

It solves the linear or nonlinear equations resulting from the assembly of the elements, providing a set of raw results that are the values of the unknown magnitude in all the nodes of the cutting. The post-processor then takes up these results, which are stored in an output file.

I-4 the post-processor

It is a graphical program, which allows to visualize the results of calculation of the fields obtained by the Solver in the form of graphs. Among other things, it makes it possible to trace the equipotential or the flux lines. The interactive interface of the post-processor can work in three different modes.

- In raster mode, the user can inspect the field values in any point of the domain being studied.
- In contour mode, the user can record and plot along a predetermined contour various field quantities such as the vector potential, the normal components and tangential magnetic flux and magnetic field, the flux, and determine the produced force or torque generated ... etc.
- Block mode allows the user to define a subdomain in a region, whose solution is an amount of surface integrals or volume. These integrals include magnetic energy, co-magnetic energy, and inductance, different types of losses, total current and torque.

In addition, the Lua compiler has been integrated into the FEMM software to allow the user to create programs, written in Lau language, facilitating the construction and analysis of geometries as well as the evaluation of the results of the post-processor.

The software allows to reach concrete solutions, it is applicable for the analysis of the electrical behaviors below :

- Magnetism: calculation of electrical and magnetic quantities due to magnets, imposed fluxes, continuous or variable currents, imposed or induced.
- Electrostatics: steady-state calculation of potentials and electric fields with or without flow of currents in dielectric or conductive media.
- Thermal: calculation of the distribution of temperatures created by powers dissipated temperature differences or heat fluxes.

The layout of a given geometry is usually done in four steps, not necessarily Sequential:

- Place the nodes defining the field of study.
- Connect the different nodes with each other by segments of lines or arcs according to the geometry of the domain to be drawn
- Assign to each geometric predefined region the material that corresponds to it (air, iron, permanent magnets…etc.), as well as the size of the associated mesh. The software has a library of materials that can be enriched by the user.
- Define the schema or data sources (direction and direction of magnets)
- Indicate the boundary conditions on the specific boundaries of the field of study...

The domain thus obtained, consisting of a certain number of different media, is discretized into small elements by a triangular mesh, each triangle being marked by its three vertices. In each element, the vector potential is approximated by a polynomial of the first degree.

In addition, the LUA compiler has been integrated into the FEMM software to allow the user to create programs, written in LUA language, facilitating the construction and analysis of geometries as well as the evaluation of the results of the post processor. In addition, the LUA compiler, allowing mathematical equations or expressions to be introduced instead of numerical values, analyzes all the dialog boxes of the FEMM software.

LUA source code, as well as detailed documentation about programming in LUA language, can be obtained from http://www.lua.org.

II- Finite element analysis

A radial field magnetic gear of the CVT, whose main design parameters are given in Table II, has been analysed employing 2D finite element (FE) analysis. Since the back iron of the control rotor essentially isolates the magnetic fields in the air-gaps of the brushless machine and the magnet gear, an FE model of the three rotors inside the back iron is sufficient for quantifying the torque transmission capacity.

We took the example of Figure 1 and we did it under FEMM for the study of magnetic induction and torque.

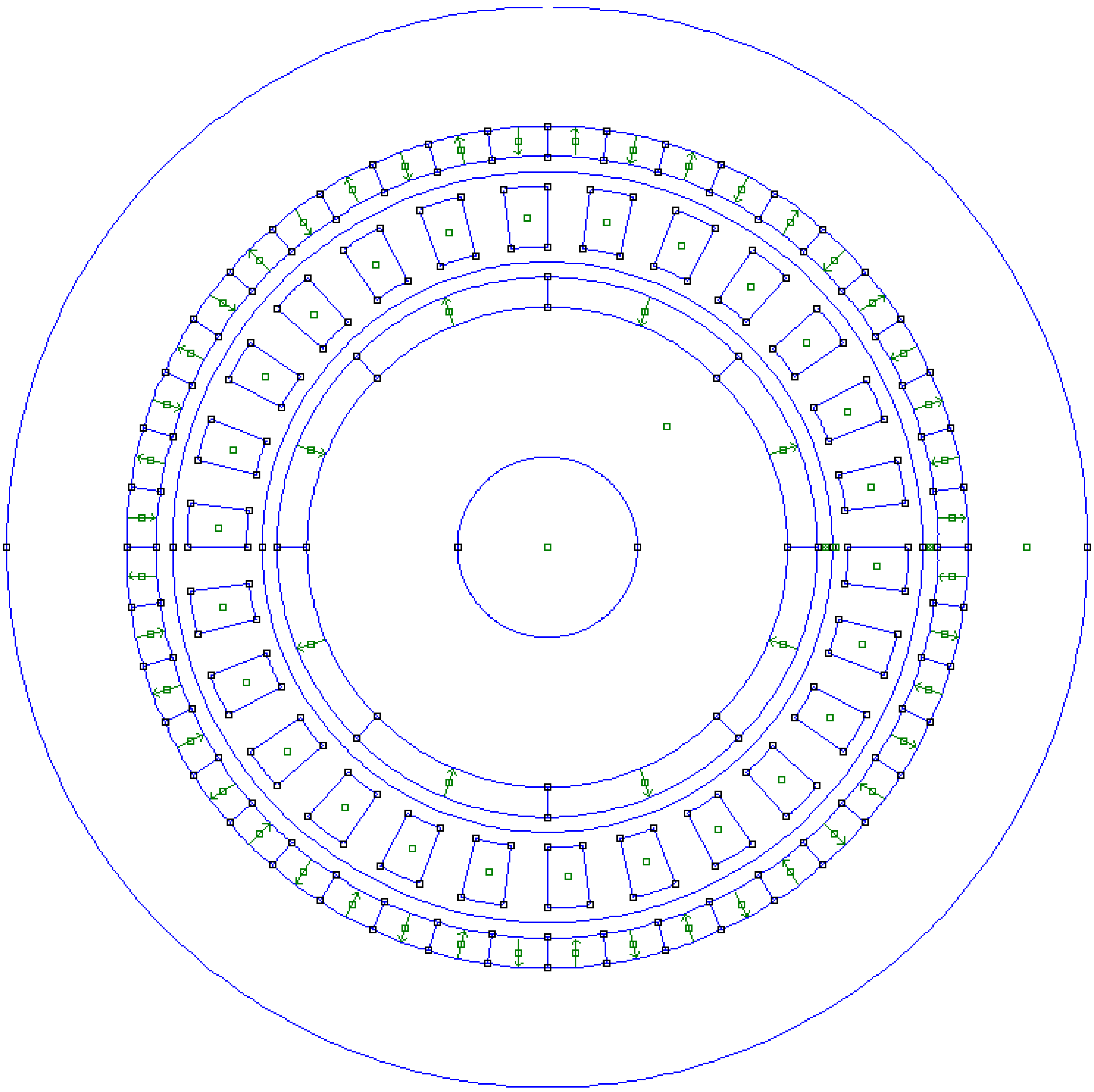

Figure –XXVI-model of magnetic gear

Outer radius of control rotor	70 mm
Inner radius of input rotor	35 mm
Radial thickness of magnets	04 mm
Radial thickness of pole-pieces	7.5 mm
Number of pole-pairs in the input rotor Ph	04
Number of pole-pieces in the output rotor ns	26
Number of pole-pairs in the control rotor Pl	22
Air-gap length	03 mm
Type of magnets	NdFeB MGOe 40

Table –II-design parameters

II-1 study of electromagnetic torque:

In this part, we will study the torque exerted on the inner and outer rotors.

II-1-1 torque exerted on inner rotor

To calculate the torque exerted on the inner rotor, the control rotor is fixed and the inner rotor is rotated, we obtain the following curve:

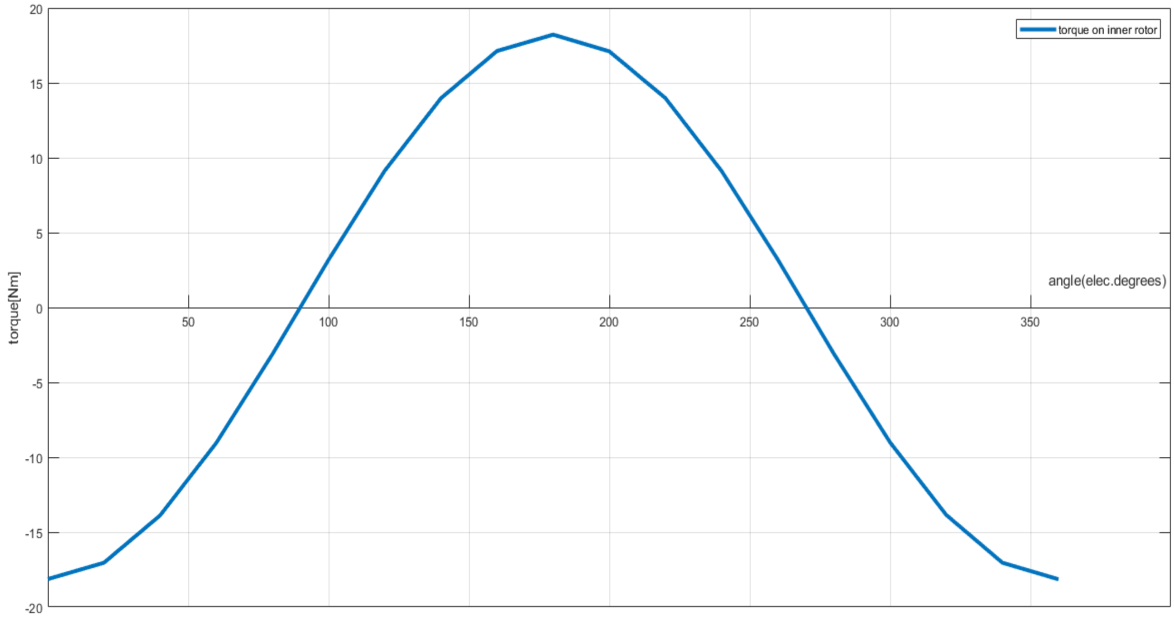

Figure –XXVII-E-magnetic torque on inner rotor

In the case of the internal rotor, an electric period is equal to 90 ° in mechanical angle because the inner rotor carries 04 pairs of poles.

The maximum torque that can reach the gear at the inner rotor is 18 Nm

II-1-2 torque exerted on control rotor

To calculate the torque exerted on the control rotor, the inner rotor is fixed and the control rotor is rotated,

Which gives us the following curve:

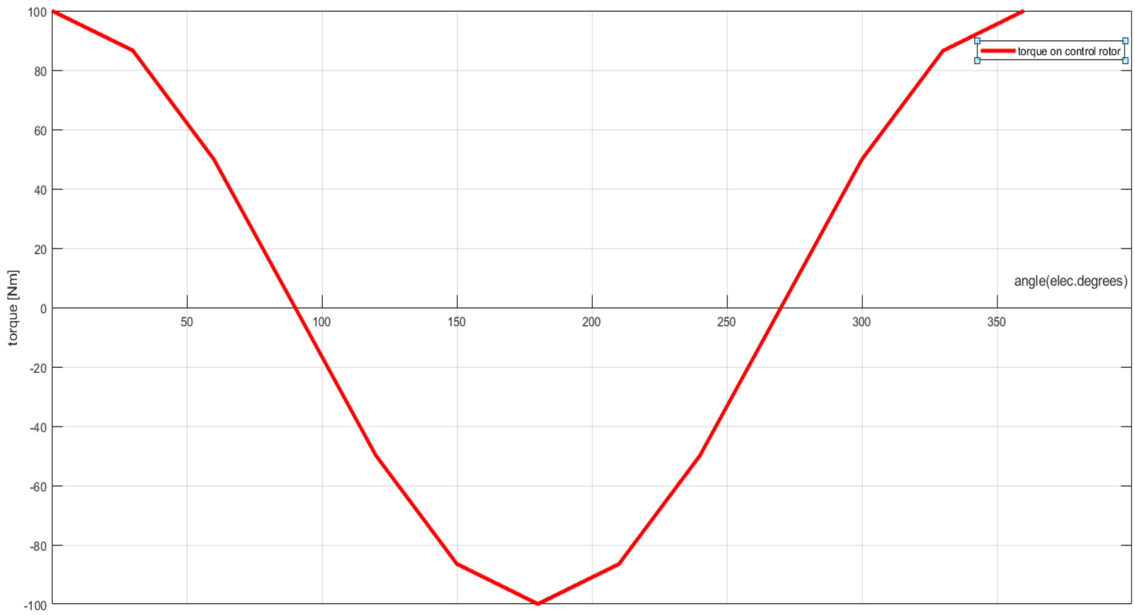

Figure –XXVIII-E-magnetic torque on control rotor

In the case of the control rotor, an electric period is equal to 16.36 ° in mechanical angle because the control rotor carries 22 pairs of poles.

The maximum torque that can reach the gear at the inner rotor is 99 Nm.

By embedding the two figures (XXVII and XXVIII) of the torque of the inner and outer rotors on a same plan, it allowed us to obtain the following figure:

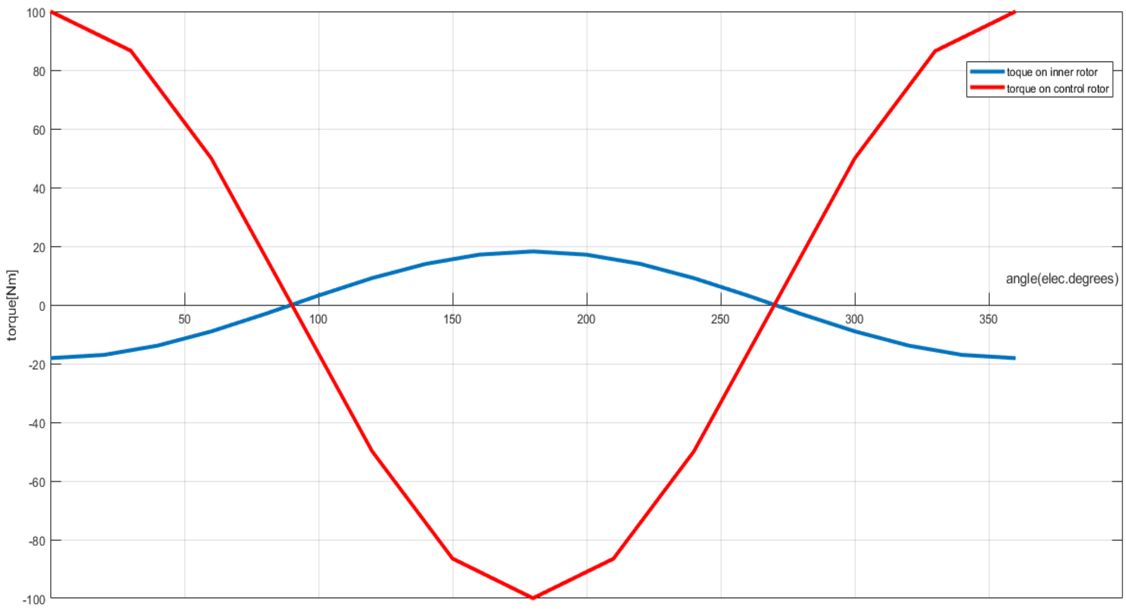

Figure –XXX-torque on inner and control rotor

The values of the internal and external torque are of different sign, this is explained by the fact that the two rotors rotate in two different directions.

By observing the values obtained, it is noted that the gear ratio is clearly distinguished, which is 5.5

II-2 study of magnetic induction

We will study the magnetic inductions by going through two steps that will allow us to calculate the induction for each internal and external gap respectively.

II-2-1 magnetic induction in the inner airgap

We replace the permanent magnets at the control rotor with air in order to have the induction at the inner air gap, a point is fixed in the inner air gap and induction is started by rotating the internal rotor.

This gives the radial induction created by the internal magnets as shown in Figure XXXI.

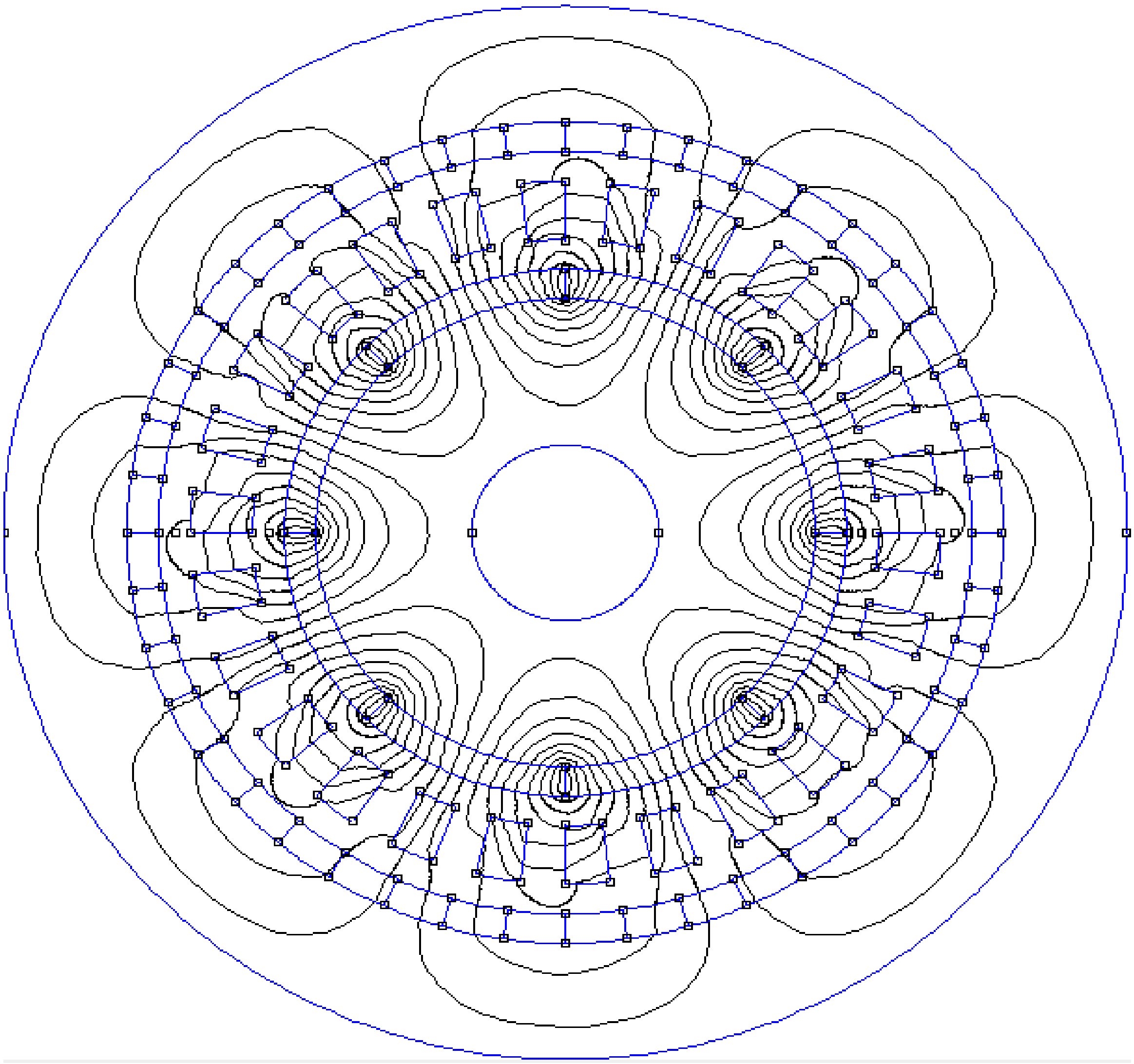

Figure –XXXI- Field lines created by the inner rotor magnets

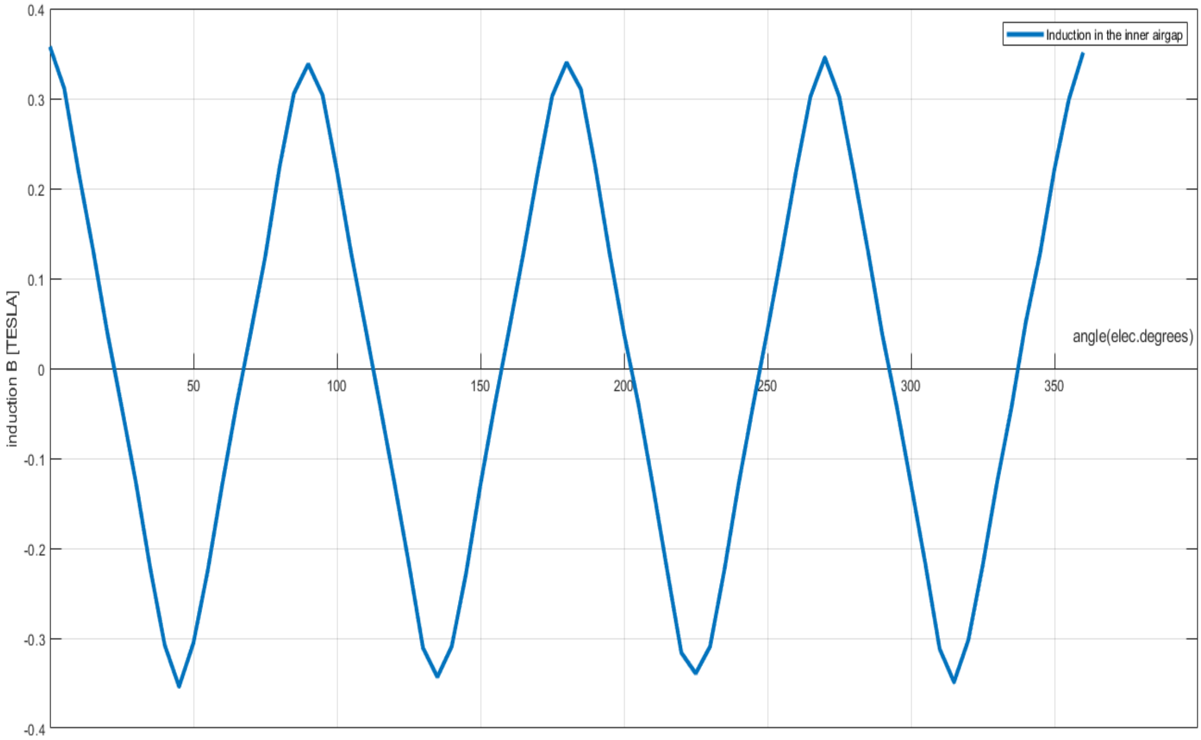

Figure -XXXII-magnetic induction in the inner air-gap

From the curve obtained from the found values, we observe that the induction reaches the peak value of 0.35T (tesla).

II-2-2 magnetic induction in the outer airgap

In this second step, we will reintroduce the permanent magnets to the outer rotor and replace those of the inner rotor with air while fixing a point at the external air gap in order to have the radial induction by rotating the rotor external like given in Figure III.9.

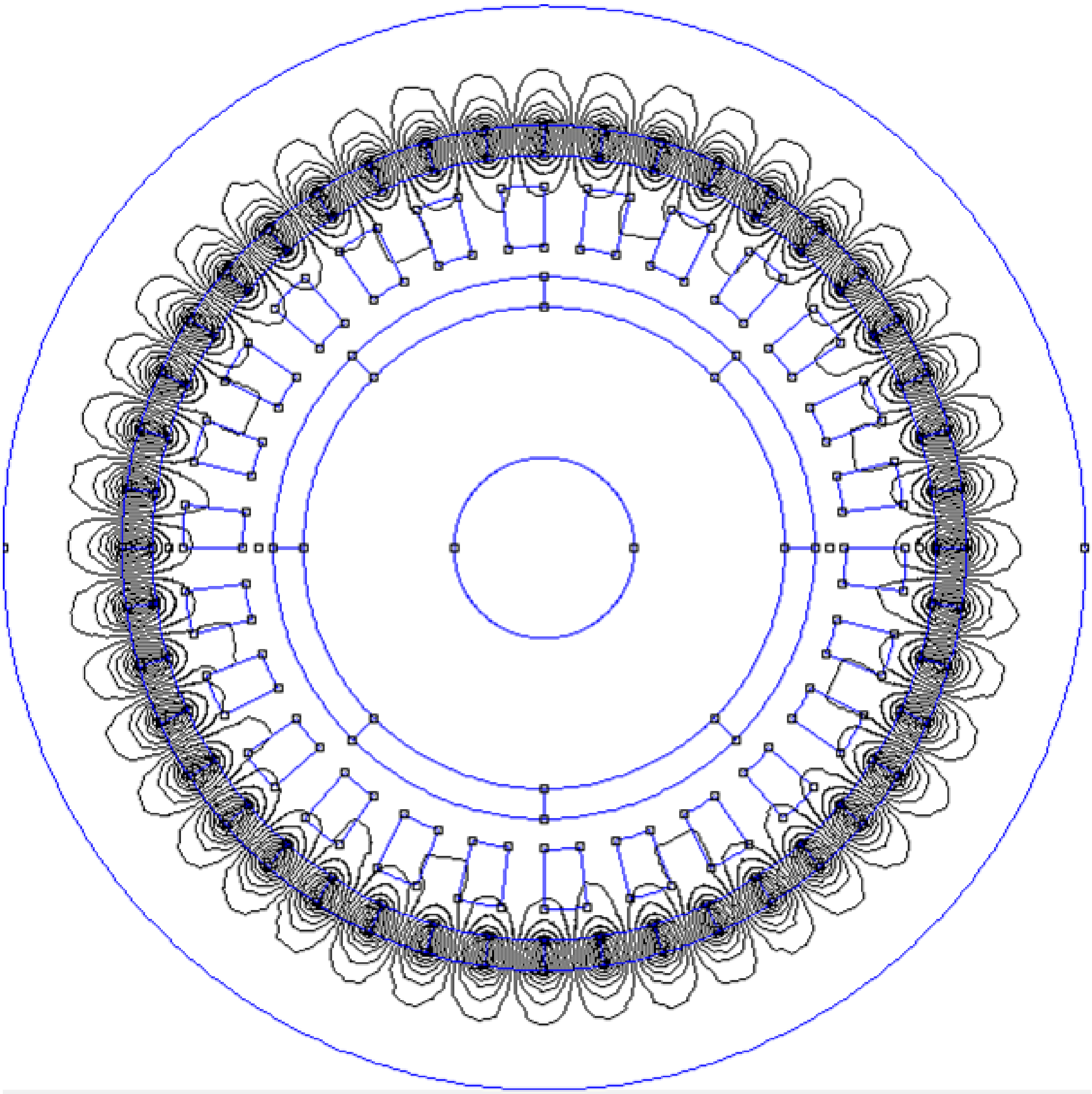

Figure -XXXIII- Field lines created by the control rotor magnets

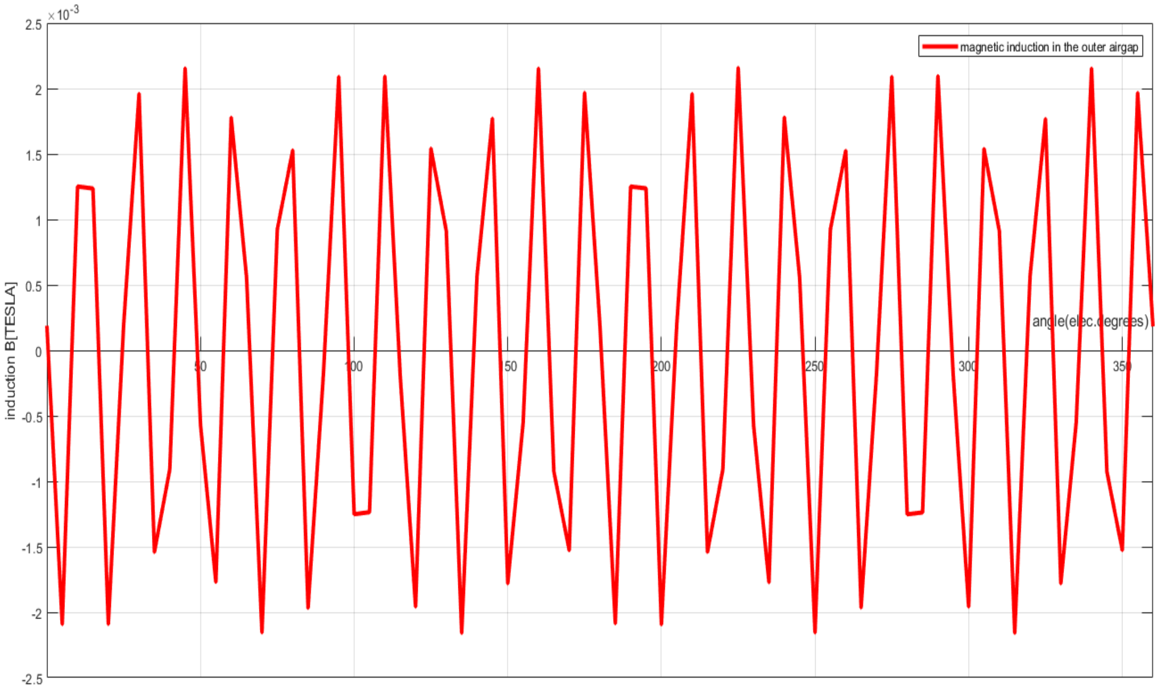

Figure -XXXIV-magnetic induction on outer air-gap

According to the curve given by the calculated values it is observed that the peak value for the magnetic induction at the outer gap is 0.0025T (tesla) for the same type of magnets as that used for the inner rotor.

III- Conclusion

After modeling a magnetic gear system under FEMM, we have shown that the torque transmitted between the rotors varies sinusoidally with the angle mentioned. We have also shown that the transmission ratio is the same as that calculated.

By integrating this magnetic gear with a brushless PM machine, it is possible to realize a continuously variable transmission device. Compared to other CVT technologies reported to date, magnetic CVT has many advantages in terms of efficiency, reliability, reduced maintenance and inherent overload protection, etc. An analytical expression to govern the transmission of the torque.

Tasdawit n Bgayet
Université de Béjaïa

SAPIENZA
UNIVERSITÀ DI ROMA

General conclusion

The work presented in this thesis deals with the study of magnetic gears, for the realization of a prototype.

At first, we made state of the art magnetic gears as well as their evolutions over time, their advantages and the different fields of application or this kind of technology can serve.

In a 2nd time, we looked at the equations that govern the magnetic gear based on the work of Attalah, the possibility of making the magnetic gear as efficient as a mechanical gear is proved by playing on the number permanent magnets and polar pieces.

We are particularly interested in the mCVT which is a variable magnetic transmission giving an electrically controllable speed ratio. The mCVT is of particular interest as a very efficient power-sharing device for hybrid parallel hybrid vehicles, but also has potential applications in renewable energies, marine propulsion.

Attalah's work allowed us to transmit the mechanical equations governing CVTs.

Finally, we made a magnetic gear under FEMM for integration into a PM machine. We studied the magnetic induction as well as the transmitted torque.

In future work, we would like to realize a complete CVT to be integrated into the wheels of an airplane in order to recover the kinetic energy created by the braking during the landing and to reuse the latter during take-off

جامعة بجاية
Tasdawit n Bgayet
Université de Béjaïa

SAPIENZA
UNIVERSITÀ DI ROMA